Validation and extension of a biomechanical model of wheelchair propulsion

by

Michael Lee Hofstad

A Thesis Submitted to the
Graduate Faculty in Partial Fulfillment of the
Requirements for the Degree of
MASTER OF SCIENCE

Interdepartmental Program: Biomedical Engineering
Major: Biomedical Engineering

Iowa State University
Ames, Iowa

1992

TABLE OF CONTENTS

LIST OF FIGURES

LIST OF TABLES

INTRODUCTION

The focus of most wheelchair research in recent years has dealt with various aspects of racing and competitive sport wheelchairs. New age technologies are used to research propulsion techniques and cardiorespiratory responses of the user. In addition, other studies have concentrated on wheelchair design for improving the efficiency of propulsion. The results of these advances have led to the production of new materials for lightweight wheelchair construction and provided new wheelchair designs which have given racers a competitive edge.

While it is important that this research continue to progress, it is also necessary to make sure that everyday wheelchair users benefit from these advancements as well. The purpose of this project was to help bridge this gap and further develop criteria for prescribing wheelchairs by studying the dynamics of standard wheelchair propulsion. Mathematical models of racing wheelchairs, which have yet to be validated, were obtained from the literature and used as a starting point in attaining a valid model of standard wheelchair propulsion.

The models used in this study were from separate works done by Cooper (1990c), Niesing et al. (1990), and Johnson and Aylor (1985). The first two models are linear first order differential equations written for a racing wheelchair in two dimensions. Dr. Johnson's model is a complex system of differential equations written for an electric wheelchair but contains some useful sections which model the effects of environmental factors on wheelchair propulsion.

The study of wheelchair dynamics with these three models involves the force required to propel the wheelchair across the floor, the resulting acceleration, velocity and distance traveled. The mathematical models equate the force with the acceleration

of the wheelchair and the environmental factors resisting motion: air drag, rolling resistance, bearing resistance, and the slope of the ground. Actual measurements of the wheelchair dynamics were experimentally obtained and used as input into the models assuring that the force calculated is significantly similar to the force measured.

Experimental measurements of the wheelchair dynamics were recorded while subjects propelled a wheelchair across the floor. The force was measured by a load cell while the acceleration was obtained via digitization techniques of a video tape recording of the event. The force and acceleration data were processed separately and then statistically compared.

Obtaining a valid model for wheelchair propulsion is the current step in the development of an extensive three dimensional model of the wheelchair, environment, and subject. It is desired to know to what extent each of the environmental factors contributes to the model as a whole. Questions to be answered included which factors play a significant role and which factors, if any, were negligible. Immediate outcomes of this validation include an accurate description of the force required of an individual to propel a wheelchair of given specifications. By knowing the physical capabilities of a person, a certain wheelchair may or may not be prescribed based on the force prediction during simulation. After a valid model has been attained, it will be possible to begin developing and combining a subject model with the wheelchair model.

LITERATURE REVIEW

In the area of wheelchair dynamics, much research dealing with all kinds of wheelchairs has been published. The following literature review discusses this research in an attempt to describe the dynamics of standard wheelchair propulsion. There are four sections to this chapter: The first section demonstrates the development of each of the three dynamic models of wheelchair propulsion and includes the assumptions made and the purposes of each model. The second section breaks down the various components of the models to show how each segment contributes to the whole equation. The third section discusses various wheelchair design characteristics and how they affect propulsion. The final section shows four methods of studying wheelchair motion, demonstrating the advantages and disadvantages of each.

Wheelchair Models

Several researchers have developed mathematical models that describe the dynamics of a wheelchair. Because each researcher has a different purpose and assumptions, the mathematical models have various components. However there are numerous underlying similarities amongst the models including the consideration of rolling resistance, air drag, and the slope of the floor. In order to transform these models into a model of standard wheelchair propulsion, it was necessary to look at the purposes, the assumptions, and the development of each of three different models.

Model of racing wheelchair propulsion

In an effort to improve the performance and efficiency of racing wheelchairs, Cooper (1989, 1990b, 1990c, 1991) developed computer and mathematical models of racing wheelchair propulsion. The combination of the models in this paper represents

the entire human/machine system including the physiological aspects of the user, the biomechanics of propulsion, the wheelchair dynamics, and the influence of the environment on the system. Cooper modeled these systems in order to study the factors which affect performance and the interactions of the user with the wheelchair.

The greatest concern in this paper was the model of the racing wheelchair and the effects of the environment. The concept of this model was that the wheelchair can be described as a linear system which converts the input forces at the push-rings into an output velocity of the center of mass. To simplify the model the authors assumed that the roll axis is parallel with the center line of the wheelchair, a valid assumption as long as the wheelchair is propelled in a straight line. The resulting model is two dimensional; the force generated in the equation was the total force of both the left and right sides. Equation 1 was derived by summing all of the external forces acting on the wheelchair.

$$F*(R/r_{pr})=(M+I/R+I_f/r)*a+C*v^2+K*v+(W_R*b_R/R+W_r*b_r/r)*\cos\theta(x)+W*\sin\theta(x)$$

Equation 1

where:

F = force tangent to push-ring
a = wheelchair acceleration
v = wheelchair velocity
x = distance traversed
R = radius of rear wheels
r = radius of front wheels
r_{pr} = radius of push-rings
I = inertia of rear wheels
I_f = inertia of front wheels
C = drag coefficient
K = coefficient of bearing resistance
b_R = coefficient of rear rolling resistance
b_r = coefficient of front rolling resistance
M = weight of individual and wheelchair
W = weight of individual and wheelchair
W_R = weight on rear wheels
W_r = weight on front wheels
$\theta(x)$ = angle of inclination

In this model, the force applied tangent to the push-ring is multiplied by the gear ratio (R/r_{pr}) of the wheel to the hand rim to represent the mechanical advantage of the user. The factor $(M + I/R + I_f/r)*a$ describes the acceleration of the wheelchair. The environmental factors considered were modelled as follows:

$$\text{rolling resistance} = (W_R*b_R/R + W_r*b_r/r)*\cos\theta(x) \qquad \text{Equation 2a}$$

$$\text{effect of slope} = W*\sin\theta(x) \qquad \text{Equation 2b}$$

$$\text{bearing resistance} = K*v \qquad \text{Equation 2c}$$

$$\text{air drag} = C*v^2 \qquad \text{Equation 2d}$$

This model of wheelchair dynamics and environmental influence developed by Cooper (1990c) has yet to be verified and was one of the models examined in the present study for understanding the dynamics of standard wheelchair.

Computer-controlled wheelchair ergometer model

As part of a large project Niesing et al. (1990) developed a wheelchair ergometer and a mathematical model for physical and computer simulation of wheelchair propulsion. The ergometer consisted of the various wheelchair components assembled on a frame in such a way that each piece was adjustable. An adjustable control system provided accurate simulation of rolling resistance, air drag, wind speed, and slope. In addition, force transducers were placed in the seat, backrest, side frames and hand rims to determine the forces involved during propulsion. The approach used by Niesing et al. (1990) was that by understanding the biomechanics of the wheelchair and physiological measurements of the user, the ability to manipulate conditions of real-life propulsion makes it possible to analyze the wheelchair/user interface. The physiological measurements desired included the applied workload, the forces applied

by the user to overcome this workload, and the metabolic cost of performance (Niesing et al., 1990).

Although there were no stated assumptions for this model, it was developed for wheelchair propulsion and testing on the ergometer. It is therefore an implicit assumption that the ergometer is an accurate representation of a wheelchair in real-life use. To verify this claim, an experiment was performed comparing subjects on both a motor-driven treadmill and the ergometer under theoretically similar conditions. The validity of measurements using the wheelchair ergometer was based on close agreement between cardiorespiratory data of the subjects on each device (Niesing et al., 1990).

The ability to solve the mathematical model depends on the measurement of the force applied to the hand rims during motion. This force was resolved into three directions: tangential, radial, and axial. The only force that contributes to forward motion of the wheelchair is the tangential force with the other two forces seen as mechanical losses. Niesing et al. (1990) developed a series of equations which use F_h as the tangential component of the force applied. Once F_h is great enough to overcome stationary rolling resistance, the wheelchair begins to roll and is influenced by the inertia of the wheelchair/user system, the rolling resistance F_r, the air resistance F_a, and the slope F_α. The resulting force, F_t, on the wheelchair is:

$$F_t = (F_h * R_h/R_w) - F_r - F_a - F_\alpha \qquad \text{Equation 3}$$

where R_h is the radius of the hand rim and R_w is the radius of the rear wheel. The equation of motion comes from this and is shown as equation 4.

$$F_t = (W/g) * a \qquad \text{Equation 4}$$

where W and a are the weight and acceleration of the system, and g is the effect of gravity. By measuring the torque applied to the wheels on the ergometer and using the values for F_r, F_a, and F_α, integration of equation 4 gives the momentary velocity of the wheelchair.

$$v = \int a dt = \int [(F_t * g)/W] dt \qquad \text{Equation 5}$$

In order to determine the validity of the ergometer, subjects were compared on both a motor-driven treadmill and the final design of the ergometer under theoretically equal conditions. Results of cardiorespiratory data showed good agreement between the devices. In addition to this test, two pilot studies were performed testing the capabilities of the ergometer itself. To date, there have been no published results pertaining to the validity of this mathematical model.

Electric wheelchair model

The electric wheelchair model was a complex, analytical representation of wheelchair dynamics and was developed as a stepping-stone for wheelchair designers (Johnson and Aylor, 1985). The complexity of this model was a result of the high standards set for its use. It was used in the present study for the factors modeling air drag, rolling resistance, and axle friction.

The purpose of the Johnson and Aylor model and resulting simulation package was to complete one step of a process towards the development of an automatic guidance system for wheelchairs. For this type of system to be successful, a complete understanding of the dynamics of a typical wheelchair is needed. Other researchers have modelled straight paths to simplify the dynamics; however, an automatic guidance system must consider steering for safe operation. The model was further complicated

by the fact that it was for an electric wheelchair. Since the driving forces are generated by a motor, they were simulated in terms of individual motor currents and voltages.

In the development of this model three assumptions were made:

1) only motion on flat, smooth surfaces was considered. There could be a slope, but no bumps or holes.

2) load transfers within the wheelchair system produced a negligible amount of physical tilting since the wheelchair lacks a spring system. They were not implying that load transfers do not significantly affect the location of the center of mass, the external forces, and the moments acting on the wheelchair.

3) each wheel of the chair experiences enough frictional contact with the floor surface to prevent slippage.

For the purpose of an automatic control system, surfaces used were typical indoor floors, and the above assumptions were considered valid (Johnson and Aylor, 1985).

The models of the different external forces were developed individually, but were defined as a single force for simulation purposes. The equation below represents the force required to overcome rolling resistance, axle friction, and air drag for each wheel i and is only a portion of the model developed.

$$F_i = (c + R_{axi} * C_{ax}) * (N_i/R_i) * \mathrm{sgn}(\theta_i) + K_a * V_o \qquad \text{Equation 6}$$

where:

c = coefficient of rolling resistance
C_{ax} = coefficient of axle friction
K_a = coefficient of air drag
V_o = velocity of the rear axis center
R_{axi} = radius of axle i
R_i = radius of wheel i
N_i = weight supported by wheel i

The $\text{sgn}(\theta_i)$ is a function for orientation and simulation purposes and is defined as:

$$\text{sgn}(\theta_i) = \begin{cases} 1 & \theta_i > 0 \\ 0 & \theta_i = 0 \\ -1 & \theta_i < 0 \end{cases}$$

Breaking equation 6 down into its components shows that the force required to overcome each factor was modelled as:

$$\text{rolling resistance} = c * (N_i/R_i) * \text{sgn}(\theta_i) \qquad \text{Equation 7a}$$

$$\text{axle friction} = (R_{axi}) * (C_{ax}) * (N_i/R_i) * \text{sgn}(\theta_i) \qquad \text{Equation 7b}$$

$$\text{air drag} = (K_a) * (V_o) \qquad \text{Equation 7c}$$

Other external forces that needed to be modeled for the automatic guidance system to be successful included the sliding frictional forces, the frictional moments present in the wheel/surface contact region, and the driving forces of the motor. However, these forces are involved with a turning and powered wheelchair and were not considered in the present study.

To verify the model, three simulation tests of wheelchair motion on a digital computer were run in conjunction with real wheelchair tests. Experimental tests were performed with an electric wheelchair instrumented such that the rear wheel velocities and the castor orientations could be measured as functions of time. The first two simulations compared real test results with the respective computer model predictions. These simulations were: (1) generation of a deceleration curve after constant velocity of the wheelchair had been attained, and (2) determination of the caster angle step

response when the initial castor angle is nonzero. The third simulation compared model to model predictions of motion testing the hypothesis that the castor mass could be considered negligible. The results of all three simulations were shown visually in a graph to agree favorably but no tests of statistical significance were presented. Considering the castor mass negligible did not degrade the accuracy of the model, thus making the assumptions reasonable and acceptable.

Mechanical Factors Influencing Performance

The various components of the models present in the previous section dictate the amount of energy required to propel the wheelchair. The mechanical and environmental factors that resist motion include rolling resistance, bearing resistance, slope, and air drag. Although these factors have been studied in terms of the standard wheelchair, it is important to see how they fit into the wheelchair models. The following looks individually at the forces needed to overcome each of these mechanical and environmental factors.

Rolling resistance

Rolling resistance is primarily a function of wheel and castor characteristics, total weight, and weight distribution. Efforts to improve these design aspects have been somewhat successful. Recent research has shown that cross section reduces tire drag and developed new tire materials (Gordon et al., 1989; Frank and Abel, 1989). Manufacturers have used light weight materials to aid in reducing total weight. However, the mass distribution of the wheelchair, which is important to the user's balance, makes optimization more personal.

Rolling resistance occurs as a result of the deformation of the wheel and the ground surface. The tire characteristics that directly and indirectly affect rolling

resistance are the diameter of the wheel and the modulus of elasticity of the tire (Brubaker, 1986; Krepchin, 1982). During operation, the deformation of the tire, defined as the coefficient of rolling friction, ϵ, is the imaginary distance between the weight vector, W, and the normal reaction vector, N (Niesing et al., 1990). Hard tires, such as a properly inflated pneumatic tire, have a lower modulus of elasticity and will therefore have a smaller coefficient of rolling resistance. Figure 1 shows the relationship of these parameters.

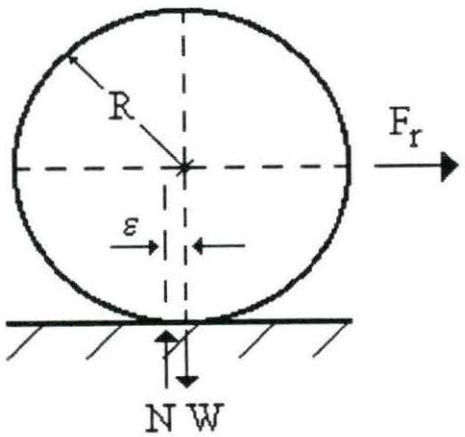

Figure 1. Definition of rolling resistance

The total weight of the wheelchair and user directly affects the force, F_r, needed to overcome rolling resistance while the radius of the wheel, R, inversely affects the resistance. Equation 8 mathematically describes this force (Niesing et al., 1990). All three models contain the rolling resistance component similar to equation 8 in which W is the weight vector and ϵ is the coefficient of rolling resistance.

$$F_r = \frac{W * \epsilon}{R} \qquad \text{Equation 8}$$

Mass distribution comes into play with the application of equation 8 to the two types of wheels on a wheelchair. With an even distribution of the load to the front castors and the rear wheels, the force, F_r, is smaller for the rear wheels because of their larger diameter. It follows that when the center of gravity is shifted rearward, the force required to overcome the rolling resistance of the wheelchair decreases; however, the rearward instability is increased. Along these same lines, by increasing the wheelbase the rearward stability increases (Lemaire et al., 1991). Conventional wheelchair mass distribution is approximately 60% on the rear axle and 40% on the front castors. By shifting the weight rearward to a 75: 25 distribution, the rolling resistance decreases by 6% (Brubaker, 1990).

While working with disabled individuals, the variety of body types poses problems for providing correct wheelchair mass distribution. An individual with lower limb amputation, for example, will have a different weight distribution and therefore a different center of gravity. An amputee will have less weight on the front castors, shifting the user's center of gravity rearward, and causing greater instability. As a result, when optimizing the rolling resistance, rearward stability must also be considered which depends mainly on the user.

In terms of applying equation 8 to wheelchair use, one must obtain information on the distribution over each wheel. One variation on this model, equation 9a and 9b, developed by Lemaire et al. (1991), incorporates the user/wheelchair system's center of gravity for determining the weight distribution over each wheel. The total weight of the system is used in the equation and adjusted by a factor equivalent to the distance from the center of gravity to the rear wheel axle divided by the wheelbase length. Equation 9a is the force needed to overcome rolling resistance of one front wheel while equation 9b is for the rear wheel.

$$F_f = \epsilon_f * (R_{cg} * W)/L_{wb} \qquad \text{Equation 9a}$$

$$F_r = \epsilon_r * [W - (R_{cg} * W)/L_{wb}] \qquad \text{Equation 9b}$$

where: ϵ_f = coefficient of front wheel rolling resistance
ϵ_r = coefficient of rear wheel rolling resistance
R_{cg} = distance from the rear wheel axle to the center of gravity
W = total weight of the user and wheelchair
L_{wb} = wheelbase length

Although Lemaire et al. (1991) outline a procedure for finding the center of gravity, a quick estimate can be obtained from results of their measurements on a test dummy (ISO Standard 7176 - 11). The dummy weighed 100.00 kilograms and had a center of gravity 17.1 centimeters from the rear axle. A conversion factor of 0.171 was be used to estimate R_{cg} for a subject's weight. The accuracy of this estimation depends on the body type of the subject.

Two additional factors contributing to rolling resistance are the surface texture and surface slope involved. The characteristics of the surface have similar effects on

the rolling resistance of the wheelchair as do tire characteristics. Smooth, hard, polished floors are easier to drive across than a carpet or even outdoor concrete sidewalks (Gordon et al., 1989).

Obviously, the slope of the ground is going to affect the work required to move up it, down it,or across it. This added force is related to the total weight of the system and the angle of the slope. In other words:

$$F_{slope} = W * \sin\theta \qquad \text{Equation 10}$$

where W is the weight of the wheelchair/user and θ is the angle of the road. Upward slope is indicated as a positive angle (Niesing et al, 1990).

Bearing resistance

It is easy to understand why the force required to overcome bearing resistance is rarely mentioned in wheelchair literature after noticing how complicated calculating the force actually is compared to its small magnitude. As with a bicycle wheel or similar device, the ball bearings used in wheelchairs transfer forces from the rotating wheel to the stationary chair components and permit translation of the wheelchair (Harris, 1984; Phillips, 1988). The force generated by gravity and propulsion is transferred through the ball/raceway contacts causing bending and localized deflections in the bearing rings (Phillips, 1988).

Although ball bearings are sometimes called antifriction bearings, small amounts of frictional power are lost during operation. Any magnitude of friction represents an energy loss and causes a retardation of motion. This energy loss is generally measured as a retarding torque. A temperature rise of the structure and the lubricant occurs unless the frictional heat is effectively removed or naturally lost (Harris, 1984).

Of the numerous components that constitute frictional resistance in the ball bearing system, sliding friction in the contact area is the most significant. Sliding occurs in bearings due to the basic internal geometry of the bearing (Harris, 1984). Other factors contributing to frictional resistance include the speed of rotation, the clearance between the axle and the bearing, and the viscosity of the lubricant (Beer and Johnston, 1984).

For the purpose of analysis, the coefficient of friction, μ, is considered a constant and defined as:

$$\mu = \frac{\tau}{\sigma} \qquad \text{Equation 11}$$

where τ is the surface shear stress and σ is the normal stress of the contact surfaces (Harris, 1984). These stresses are the result of the axle "climbing" in the bearings as the wheel is set in motion. At a certain point the axle can no longer climb and slipping occurs. At the point of slippage, a bearing reaction vector R, just offset to the normal vector N, is developed. In order to maintain a wheel rotating at constant speed, a couple, M, must be applied. This couple represents the force required to overcome the bearing frictional resistance and is modelled as:

$$M = R * r * \mu \qquad \text{Equation 12}$$

where r is the radius of the wheel axle and R is equal and opposite in direction to N (Beer and Johnson, 1984). The relationship of M, R and N is such that the moment of M balances the moments of R and N (Beer and Johnston, 1984). The coefficient of friction of roller bearings has been shown to be between 0.0001 and 0.15, where values

in the range of 0.06 to 0.07 are most common and represent systems that appear to have neither too much sliding or too much traction (Harris,1984).

The inclusion of a factor for bearing resistance in wheelchair models is not as well accepted as the other environmental factors. Some researchers have included bearing resistance (Cooper, 1990c; Johnson and Aylor, 1985) while others have not (Niesing et al, 1990), although no one offers an explanation as to its importance in their model.

The bearing resistance term in Cooper's (1990c) model is defined as a function of the wheelchair/user's velocity (equation 2c). For simplification purposes, K*v serves as an estimate of equation 13, based on the assumption that the force to overcome the bearing resistance is proportional to the velocity of the wheelchair. Equation 13 is a derivation of equation 12 which considers the bearing resistance to be different for each wheel.

$$\text{bearing resistance} = M_B/r_{ax} + M_b/r_{axf} = K*v \qquad \text{Equation 13}$$

where: M_B = bearing resistance of the rear hubs
M_b = bearing resistance of the front hubs
r_{ax} = radius of the rear axle
r_{axf} = radius of the front axle

No value for K, nor any validation for K*v as an accurate representation of bearing resistance was provided (Cooper, 1990c). Equation 13, along with the model of bearing resistance described by Johnson and Aylor (1985) as shown in equation 7b, include the radii of the wheel inversely proportional to the bearing resistance to determine how M (from equation 12) will equate into a total force for wheelchairs.

With the development and use of sealed ball bearings on wheelchairs, maintenance has been significantly reduced resulting in less care needed to maintain low bearing resistances. These bearings never require adjustment and are protected against the entry of dust, dirt and water, all of which increase friction in the bearings. The axle itself is highly stressed, especially when bouncing over bumps and holes. Currently, there are two types of axles available, the fixed bolt and the quick release, each having their advantages. The quick release offers easy removal of the wheels for storage, transports or for changing to a different wheel. The fixed bolt is attached in a more permanent manner with little room for assembly error (Brubaker, 1990).

Air drag

In an effort to determine the aerodynamic characteristics of a conventional wheelchair, an experimental study was conducted at the Longley V/STOL wind tunnel. The study included testing for the effects of wheelchair components, the effects of an occupied wheelchair, and the effect of air currents generated between the ground and the wheelchair. This information is required for a better understanding of wheelchair propulsion and must be considered in the design of new wheelchairs where increasing mobility is concerned (Coe, 1979).

The results of the study showed that the aerodynamic drag coefficient, C_D, of a wheelchair is equal to 0.96. Using a manikin the size of a fiftieth percentile man seated in the wheelchair, C_D was equal to 1.4. Using a range of free-stream dynamic pressures, the drag coefficient remained essentially constant (Coe, 1979).

The force to overcome the effects of wind drag is typically modelled as the air resistance, F_a, and is proportional to the frontal area of the wheelchair /user system and the square of the relative air speed. It can be stated as:

$$F_a = \frac{1}{2} * D * (V_w - V_1)^2 * A * C_D \qquad \text{Equation 14}$$

where: D = density of air (1.23 kgm^{-3} at STP)
V_w = velocity of the wheelchair
V_1 = velocity of the wind
A = frontal area of the wheelchair/user system
C_D = drag coefficient

The wind speed is considered negative if V_1 is a head wind and positive with a tail wind. (McLaurin and Brubaker, 1991; Niesing et al, 1990).

To test the accuracy of the drag coefficient, several additional tests at Longley Research Center were conducted. Ground effects were tested by positioning the wheelchair 2.54 cm (1.0 inch) above the wind tunnel floor. Compared to the drag coefficient of the wheelchair on the floor, the ground effects were negligible and ignored (Coe, 1979).

A similar test was done with the manikin dressed in tight clothes versus loose clothes. The difference between the fit of the clothes was minimal and their average is the stated value of $C_D = 1.4$ (Coe, 1979).

A comparison of the wheelchair component drag effects was also performed. By starting with just the frame, the drag coefficient was determined. Subsequent tests after the addition of the wheels, arm rests, leg rests, and the back rest resulted in increased drag. The effect of the adding on the back rest showed the largest increase in drag. By designing a new backrest, air drag was reduced. However, when the manikin was placed in the wheelchair, the drag coefficient returned to the original value (Coe, 1979). This demonstrates that in standard wheelchairs where body positions are more upright, air drag remains fairly constant.

Wheelchair Characteristics Affecting Propulsion

To coincide with the mechanical developments of improving wheelchair propulsion, research has also been conducted on the interface between the wheelchair and the user. Investigations of design variations involve how the seat position, hand-rim diameter, and rear wheel camber of the wheelchair affects the energy cost, cardiorespiratory response, propulsion technique, and mechanical efficiency of the user. Although the design variations are discussed separately in the following paragraphs, it does not imply that their influences act independently on the user.

Seat position

Optimal performance of wheelchair propulsion at minimal energy cost can only be attained when the wheelchair-seat configuration and the propulsion mechanism comply in an optimum manner to the functional characteristics of the user. In general, trial and error procedures are applied to fit the individual to the wheelchair in terms of vertical and horizontal placement, as well as angulation of the seat and backrest since an experimental based fitting criteria is currently unavailable (Van der Woude et al., 1989). Research has aided the prescription process by studying seat configurations, trends in propulsion mechanisms and physiological responses.

Van der Woude et al. (1989) studied seat height as a function of elbow angles (100°, 120°, 140°, and 160°) measured with hands top-dead-center on the hand rim. Results showed that the cardiorespiratory response, including oxygen cost, ventilation, and heart rate for given work loads on a treadmill, increased with increasing seat height. Minimum response values were in the 100° to 120° range of elbow extension indicating that lower seat heights were closer to optimal.

In terms of propulsion mechanics, when the seat is high the hand cannot reach as far down the rim and the push duration will be shorter. To maintain a given speed, the

cycle frequency must increase, causing an increased cardiorespiratory response. On the other hand, a low seat allows for a longer stroke over a larger section of the rim. From a mechanical point of view, a longer distance of stroke requires less force input for maintaining a given power output. Less force required results in a decreased physiological response (McLaurin and Brubaker, 1991).

The results of a study by Walsh et al. (1986) showed no significant difference in the maximum velocity attained at nine different seat positions. Motion of the trunk/upper body allowed subjects to lessen the negative effects of poor seating. Although physiological changes of the subjects were not investigated, it is reasonable to infer that the cardiorespiratory response would increase with greater trunk/upper body motion. However, differences in responses may only occur at submaximal work loads such as daily activities and not have much significance in all tests at maximal effort.

The actual success of wheelchair racers and their seat position studied by Higgs (1983) showed some characteristics that can be applied to daily use activities as well. In general, wheelchairs designed for sprinting that attained the greatest success in racing had seats that were horizontally forward and significantly higher. This forward position allowed the racer to generate higher cycle frequencies and therefore produce higher speeds. On the other hand, distance wheelchairs had rearward and lower seat positions for a longer force application.

Considering all of these studies, it can be concluded that the wheelchairs allowing low elbow angles (around 100°) with rearward placed seats are optimal. This position will keep the cardiorespiratory response lowest and is ideal for long days in the wheelchair, corresponding to the activities of distant racers. This analysis is also consistent with what was demonstrated previously with decreasing rolling resistance by moving the center of gravity closer to the rear axle.

Rear wheel camber

Inward tilted rear wheels or camber has gained much popularity for daily use wheelchairs. The advantages to rear wheel camber come from the increased distance between the contact points of the tires, and from the inward tilt at the top. The results are better lateral static stability, lower downward turning moment on a side slope, and easier to reach hand rims. Rear camber however, is not without some disadvantages. The wide wheelbase makes it more difficult to maneuver through tight doorways or corners. It was expected that camber would reduce rolling resistance and the physiological response, but the results of tests revealed that these factors were not as significant as had been expected.

In an attempt to find out what effects camber had on propulsion, Veeger et al. (1989) studied physiological responses and movement patterns of subjects during propulsion using four different degrees of wheel camber. Results showed physiological parameters including heart rate, oxygen uptake, and mechanical efficiency were independent of camber. On the other hand, camber significantly affected the stroke mechanics in terms of push time and initial placement of hand on rim, but the overall cycle time for push and recovery did not change. These kinematic results did not clearly confirm the hypothesis that increasing camber facilitates arm movement (Veeger et al., 1989). The effect of camber on rolling resistance adjusted form 0 to 10 degrees was also found to be insignificant (McLaurin and Brubaker, 1991).

In the same study in which seat position was investigated, Higgs (1983) also studied camber effects on the speed of racing wheelchairs in terms of final standings of various races. Although the trend showed that racers with small angles of wheel camber had placed lower, there was no statistical significance to the difference. One reason given for these results was the high variability of cambered wheels used by the

less successful racers. The wheelchairs in this group had a mean camber of 3.24° and a standard deviation of 3.62°. By comparison, the most successful group of racers had wheelchairs with a mean camber of 7.16° and a standard deviation of 1.92° (Higgs, 1983).

At this point, wheelchair prescription in terms of rear camber appears to be based on user preferences and abilities. Neither improved rolling resistance nor propulsion efficiency as a result of increasing rear camber have been completely established. Racers have shown some higher levels of success with cambered wheels; however, individual capabilities must be considered as indicated by the large standard deviation of less successful racers. As a result, everyday wheelchair users must decided whether or not camber is desirable based on the advantages and disadvantages involved.

Hand rim diameter

Research concerning hand rim diameter has almost exclusively dealt with sport wheelchairs. General trends indicate that there is a significantly reduced cardiorespiratory response to smaller hand rims, but the propulsion kinematics remain relatively unchanged.

For racing wheelchairs, small diameter hand rims are used to gain mechanical and speed advantage. Higgs (1983) postulated that the optimum hand rim diameter for racing may be a function of variables such as the strength and skill of the athlete and demonstrated the fact that hand rim diameter varied inversely with the level of success achieved in racing. From a mathematical perspective, pushing on a fifteen inch hand rim, on a twenty-seven inch wheel, at five kilometers per hour, will produce a wheelchair speed of 9 kmph. Since racing wheelchair speeds are much higher than this, the strength and skill of the athlete is involved. A few more simple calculations show,

that as the hand rim diameter increases, the speed of the chair decreases. This displays the importance of optimizing the hand rims for the user (McLaurin and Brubaker, 1991; Brubaker, 1988).

Similar results were reported by Van der Woude et al. (1988b) in an investigation on the effect of varying hand rim size at different velocities. Five different hand rims were used ranging in size from 0.3m to 0.56m in diameter, and were tested at four velocities. Oxygen cost, ventilation and heart rate all showed significant reductions with the smaller rims while mechanical efficiency improved.

There are two possible explanations for these results. First, in order to reach small hand rims, the seat must be lowered and the wheels cambered to permit the arms to reach comfortably over the wheels. This puts the user in a compact, stream lined position offering lower air resistance and therefore less work is needed (McLaurin and Brubaker, 1991). The second explanation comes from the results demonstrated by analysis of stroke mechanics. Simply stated, the smaller the mechanical advantage (i.e. the smaller the hand rim to wheel ratio) the higher the mechanical efficiency and the lower cardiorespiratory response. At each velocity, Van der Woude et al. (1988b) showed that the push angle and cycle time did not change with hand rim size. Thus, the hands and arms must travel faster and further around the rim in the same amount of time for the large hand rims in order to maintain the set speed, consequentially increasing the cardiorespiratory response.

It is difficult to optimize hand rim size for standard wheelchairs since smaller hand rims require lower seat positions making it impractical for day-to-day activities and for proper long term posture. Prescribing hand rim diameters may fall under the same category as seat position for obtaining a shoulder to rim distance that will

optimize muscle mechanics in terms of length-force and force-velocity characteristics (Van der Woude et al., 1988b).

Methods of Wheelchair Testing

In order to study the aspects of wheelchairs described thus far, researchers have utilized various methods of wheelchair simulation. There are four basic scenarios with which wheelchairs have been studied in which environmental conditions are approximated and controlled: track evaluations, roller systems, treadmills, and simulated wheelchair. In each of these scenarios, film analysis and/or cardiorespiratory instruments are used to evaluate propulsion mechanics and the physiological responses of the subjects. The following discusses each of these four scenarios in terms of their advantages and disadvantages, and illustrates their use with examples of experiments.

Track evaluations

Field testing or evaluating wheelchairs on a track consists of the testing of the subject and the wheelchair over some distance as in a race or across a laboratory floor. The fact that field testing puts the subject in a real life situation and not a simulation is the key aspect of this scenario. However, studies are limited by the distance factor of the tests. This technique was used in the testing of elite athletes using their own racing wheelchairs (Higgs, 1983, 1984; Ridgeway et al., 1988; Coutts and Schutz, 1988) and standard wheelchair users (Mattison et al., 1989; Glaser and Collins, 1981).

Track evaluations were successfully used in the study by Higgs (1983) on wheelchair athletes. By using high speed film during actual competition, Higgs correlated the places that the competitors finished to their techniques and wheelchair designs. The advantage to this study was that the subjects were actually in a real life situation. It is impossible to simulate race-like atmosphere in the laboratory. Similarly,

there were no restrictive devices such as excess instrumentation attached to the subject or the wheelchair .

The disadvantage to the track method is the limitation of the field of view of the camera. As the athletes race around the track, filming occurs only during the few moments that they pass in front of the camera. The technology used in film digitization for these experiments did not allow the camera to pan along with the subjects.

Track evaluations used for non-athlete wheelchair users simulated real life situations in a large laboratory and took place on a surface of everyday use. Real life situation tests included varying the number of curves on a small course to represent propelling around furniture, corners, and other obstacles (Mattison et al.,1989). Studying the effects of different surfaces such as tiled or carpeted floors that the subject uses has also been done (Glaser and Collins,1981). The focus of these studies was to determine how the different environmental conditions affected the physiological responses of the subjects. In order to collect data, subjects had to stop at certain times to have their physiological responses measured since pushing lab equipment or dragging wires around the room was impractical. These studies proved to be an adequate means for studying the elderly and disabled users who can not sustain steady states on treadmills or ergometers (Mattison et al., 1989).

Wheelchair rollers systems

Wheelchair roller systems, sometimes called ergometers or dynamometers, refer to a set-up composed of one or two pairs of rollers on which the rear wheels are placed. Systems with two pairs of rollers simulate left hand and right hand propulsion whereas one pair of rollers assumes symmetric propulsion (Coutts,1990; Thacker et al.,1980). The other systems that are called ergometers consist of seats with separate

instrumented rims. This type of ergometer will be discussed later under simulated wheelchair devices.

Roller systems have proven to be valuable tools in studying wheelchair biomechanics. As with research done on tracks, studies involving rollers include dynamic analysis, the kinematics of propulsion, and physiological measurements. Complete measurement of motion is accomplished by two simultaneous procedures. First, the measurement of motion dynamics involves instrumentation attached to the rear roller which measures the torque and power output of the subject (Thacker et al., 1980). Sampled data from such instruments also provides the input for kinematic equations that calculate the distance, velocity, and acceleration of the wheelchair (Coutts, 1990). The second procedure is for studying the propulsion techniques and uses high speed film. The camera is placed perpendicular to the sagittal plane of the subject, parallel to the rear wheel axle (Veeger et al., 1989; Masse and Lamontagne, 1990). Physiological phenomenon can be measured quite easily since the wheelchair and subject remain stationary. It is not uncommon for researchers to use a combination of both procedures, in conjunction with physiological measurements, to optimize research efforts (Cooper, 1990a; Veeger et al., 1989; Walsh et al., 1986).

An advantage unique to roller systems is the ability to study the starting phase of wheelchair propulsion. Stroke kinematics, cycle dynamics, and motion dynamics can be studied as subjects perform a standing start at maximal effort. Because the wheelchair is stationary and the rollers are not motor-driven, it is easy to film the first several seconds of propulsion up to constant speed without the subject exiting the camera view (Cooper, 1990a; Coutts, 1990). Cooper (1990a) compared sprint and distance racers in order to discover the exact instant a forward force was being applied to the hand rims.

Coutts (1990) compared the propulsion techniques and acceleration profiles of sprint racers and basketball players.

A second advantage to the roller systems has two aspects. The first aspect is that the roller systems can be built to accept all kinds of wheelchairs. Subjects can use their own medically prescribed manual wheelchairs within the laboratory (Thacker et al., 1980), or athletes can use their own specially designed wheelchairs for the experiments (Coutts, 1990). The second aspect is that the front end of the wheelchair is stabilized or locked in place preventing accidental roll off. This allows researchers to study subjects of various skill levels (Thacker et al., 1980; Masse and Lamontagne, 1990).

One disadvantage to the roller system, as compared to the track, is that environmental conditions must be simulated or closely approximated. Since the wheelchair is stationary, adjustments must be made to compensate for the lack of mass inertia. Rolling resistance must be approximated by adjusting the inertia of the rollers (Cooper, 1990a). Air drag is the one force that cannot be simulated, and there is no capability for comparing propulsion on different surfaces.

Wheelchair treadmills

Motor driven treadmills are frequently used in biomechanical and exercise physiology studies of locomotion as well as for training and rehabilitation purposes. The most common use of a treadmill is to simulate over-ground running or walking. It has recently become popular with wheelchair researchers and athletes. Although there is a debate over the validity of extrapolating treadmill information to the over-ground environment, wheelchair propulsion can be simulated in a most realistic way (Van Ingen Shenau, 1980).

In wheelchair research, treadmills have typically been used as a tool in comparing differences in wheelchair design. Cinematography is used to study the

kinematics of propulsion at the same time cardiorespiratory data is collected on subjects using various wheelchairs. Researchers then compare treatments in terms of energy costs and stroke characteristics in an effort to optimize wheelchair design (Sanderson and Sommer, 1985; Lakomy et al.,1987; Van der Woude et al., 1988a).

Examples of this sort of experimentation are the sequence of studies done by Van der Woude et al. The experiments included the comparison of four different types of wheelchairs (Van der Woude et al., 1986), the effects of power output (Van der Woude et al., 1988a), the effects of different hand rim diameters (Van der Woude et al., 1988b), and the effects of seat height (Van der Woude et al., 1989c). In all of these experiments, subjects were evaluated by trend analysis of cardiorespiratory and kinematic parameters. The conclusions drawn were not always compared to over-ground locomotion but were used to answer the question of which configuration (i.e. seat position, body position, or rim size) of wheelchair/user interfaces were optimal (Van der Woude et al., 1986).

One advantage to the treadmill is the ability to measure the drag force due to rolling resistance, internal friction, and gravitation. By attaching the wheelchair to a load cell, the drag force is measured as the treadmill is motor driven without the subject propelling the chair (Brubaker, 1986). From this value, the power output of the subject is calculated as the drag force multiplied by the velocity of the treadmill and is used as a parameter for determining the efficiency of propulsion (Van der Woude et al., 1986).

Another advantage of the treadmill is the ability to control the subject's velocity. Researchers set the pace and thus the work load of the subjects. Having this control keeps the tests consistent for each subject and provides better repeatability amongst subjects. However, to do these studies, researchers rely on well trained wheelchair

athletes as subjects because they can endure the length of the tests and are familiar with treadmills.

An example of the ability to have control of the subject's speed is the study done by Sanderson and Sommer (1985) using treadmills and cinematography to extensively study the kinematic features of wheelchair propulsion. By plotting out the paths of the neck, shoulder, elbow, wrist, and trunk, they defined the most efficient propulsion techniques. This information is now used in the design of wheelchairs for user interface, and in the assessment of factors necessary to improve performance and rehabilitation.

The advantage to studying physiological responses with treadmills is that more control of the wheelchair is needed by the subjects as compared to that of roller systems. The subjects are not locked into position and so must work to keep the wheelchair straight and in position. As with the ergometers, the effects of different surfaces cannot be studied; however, treadmills can better simulate a change in slope. The only mechanical difference between treadmill and over-ground locomotion is the factor of air resistance (Van Ingen Shenau, 1980).

Simulated wheelchairs

In the last few years, researchers have been developing new systems for use in the laboratory to improve the methods of studying wheelchairs. These devices accurately measure power output and applied forces while at the same time mechanically simulate wheelchair driving as closely as possible. In addition, these devices provide for easy adaptation for the comparison of different wheelchair dimensions. As with the treadmills and ergometers, these simulated wheelchairs facilitate the measurement of physiological and biomechanical parameters of propulsion (Niesing et.al., 1990; Forchheimer and Lundberg, 1986).

In general, this type of dynamometer is made of an adjustable seat with separate, instrumented, rims. The seats, back rests and foot rests can be adjusted for height, width, and position over the axle. There are a variety of wheels that can be mounted at various widths as well (Burkett et al., 1987). Data acquisition systems collect from instrumented rims the dynamic parameters such as the resulting forces, torques, velocities, and accelerations (Niesing etal., 1990). To simulate the drag forces, there are chain or belt drives that connect the rims to variations of flywheels or electronic control devices (Jarvis and Rolfe, 1982; Niesing et al., 1990).

Ergometers of this type have been under development for a relatively short period of time and researchers have built them for their own purposes. It follows that one of their advantages is their versatility which includes the capability for multiple adjustments and the range of subjects skill levels. Jarvis and Rolfe (1982) used a simulated wheelchair rig to examine propulsion factors of children in an attempt to provide information for improvements in design. Their rig was portable so that it could be taken to the children. Using this device avoided prolong propulsion against frictional or treadmill resistances and allowed for the study of children with different disabilities and strengths.

These high-tech devices have two disadvantages. The first is that the more extensive the study desired, the more complicated the system needs to be, and the greater the cost of building it. A simple system may keep the cost down; however, there may be a sacrifice in the variety of studies that can be performed. The second problem with these devices is that a validation test must be run so that it is certain that a proper simulation is being achieved. Not only must the device reproduce the performance of a real wheelchair, but also the "feel". One way of proving these systems are valid involves subjects serving as their own controls in a real wheelchair. If cardiovascular and

respiratory parameters compare favorably, the device is typically proclaimed valid (Niesing et al., 1990; Burkett et al., 1987).

Burkett et al. (1987) designed a device that made use of a hysteresis brake to simulate over-ground propulsion. This brake produced resistance only when an external load was applied. This left a freewheel phase between the subjects' pushes. Burkett validated his ergometer with subjects serving as their own controls in a field test. Standard t-tests indicated no significant difference of oxygen consumption and pulmonary ventilation between the two experiments and formed the basis to the conclusion that their ergometer was valid.

The device designed by Niesing et al. (1990) appears to be the most complicated device made. Force transducers were placed in the seat and back rest as well as in the wheels. A custom-made software package was developed in order to process and analyze the data. In preliminary studies, the device was validated by comparing cardiorespiratory data with that of his subjects on a treadmill.

MATERIALS AND METHODS

The methods used in this project were modified from procedures reported in the literature and developed around available resources. It was desired to keep attachments and accessories on the wheelchair to a minimum to simulate real life movement as closely as possible. The experiment simulated the action of wheelchair users moving from one room to another. The various stages of motion studied were starting, constant propulsion, and stopping, all taking place at everyday wheelchair speeds.

The intent of this project was to study the dynamics of standard wheelchair propulsion, including the force applied to the push rims of a wheelchair and the resulting acceleration, velocity and distance traveled in order to obtain a valid model that predicts this motion. The wheelchair was connected to a constant resistance source with a load cell that measured the tension in the rope and produced the observed force data. At the same time, a video camera taped the motion of the wheelchair and user as they crossed the floor. From the video tape, the acceleration, velocity and distance of the process were determined and used as inputs to the models for producing the predicted force data. Statistical analysis of the combined observed and predicted data provided the means for validating the model. Nine test trials for each subject in which data was recorded were required for proper statistical analysis. These nine trials consisted of three trials of each phase of motion: starting, constant velocity, and stopping.

Subjects

Seven able-bodied subjects[1], ranging in age from 23 to 30, volunteered to propel the wheelchair for the experiment. Subject data is given in Table 1 along with means and standard deviations for the age, height and weight. The model called for mass, accelerations, and velocities and since propulsion technique was not the focus of the study, it was assumed that no experience in propelling a wheelchair was needed.

Table 1. Subject data

Subject	Sex	Age	Height (cm)	Weight (kg)
BF	Male	23	182.8	97.7
CO	Male	26	190.5	93.2
GN	Female	28	168.9	64.1
KH	Female	29	172.2	68.2
RK	Male	30	176.5	79.5
SK	Female	26	168.9	50.0
VD	Male	26	177.8	68.6
Mean		26.86	176.8	79.5
Standard Deviation		2.34	7.86	16.8

Equipment

Minigym

The device used to allow wheelchair motion while attached to a load cell was the Super2 Minigym model 500X by Mini Gym®, Inc. The Minigym is an isokinetic exercise device and was used because it offered constant resistance throughout a pull

---

[1] The use of human subjects was approved by the University Human Subjects Review Committee (APPENDIX B).

while allowing forward motion of the wheelchair. Resistance was initially set so that wheelchair movement was not greatly inhibited but enough to prevent "snapping" of the rope between propulsion strokes. This force needed to overcome this resistance was approximately 5.75 pounds.

Load cell

The load cell was integrated into the connection between the Minigym and the wheelchair. It was used as a force transducer and produced the observed data as it measured the tension in the rope during the wheelchair motion. The load cell converted the tension force it received into an electrical signal. The model used was a JP1000 load cell manufactured by Tyco Bytrex Division, Inc. and had a capacity of 1000 pounds. Strain gages electrically connected in a wheatstone bridge utilized piezoresistive characteristics of semiconductors to perform physical measurements. The load cell produced a zero output when no force was applied and worked in tension as well as in compression.

The load cell had an integral ten foot shielded cable ending with a CA3106B-14S-5P(A105) connector and a CH3102A-14S-5S(A105) mating connector. The connector pin arrangement was: A and D - excitation, B and C - signal, and E - shield. The load cell is supplied with ± 5 volts ac.

Accompanying the load cell was its power transformer and force display. This transformer converts 120 volts ac to 5 volts ac to be used by the load cell. It also processed the force signal from the load cell for an immediate needle display. The display was used only to initially set the load cell signal at zero. The force signal was taken from a separate three pin connector where pins A and B were signals and C was a ground. Because of the two pin signal output, a differential operational amplifier processed the data prior to its entering the oscilloscope.

Digital oscilloscope

To display the force profile during calibration and wheelchair tests, a Tektronix 2211 Digital Storage Oscilloscope with a serial port and plotter capabilities was used. The single force signal coming from the differential operational amplifier was sent to channel one of the oscilloscope. The settings on this channel were set at 0.1 volts/division with a sweep of 0.5 seconds/division. Three modes of storage were used at various times. Continuous storage maintained the trace on the screen as an event occurred. At the end of the event, the screen was saved allowing transfer to the computer. A reference trace was created from each static hang during calibration and was recalled for comparison with the drop test of the same weight. All waveforms on the oscilloscope screen were transferred to the computer via the serial ports at the push of the plotter switch.

Video camera and accessories

The video camera used to film the wheelchair movements was a Quasar VHS digital video recorder. It was positioned sixteen feet from the subject and orthoganal to the subject's sagittal plane. The height of the camera was positioned so that its field of view center was horizontal and at the mid-height of the subject. Filming speed was at 30 frames per second using a shutter speed of 1/1000 second. A 500 watt spot light with no overhead lighting and a black back drop produced a full illumination of the subject's sagittal plane and offered a high contrast between the subject and the background.

Wheelchair

A commercially available standard 24 inch folding wheelchair produced by Invacare®, Inc. was used by all subjects. The size specifications and measurements are found in Table 2. This wheelchair was obtained from Excel Medical in Ames, Iowa.

Table 2. Specifications for an Invacare standard 24 inch folding wheelchair

Radii: rear wheel: 24" (60.96 cm) front castor: 8" (20.32 cm) push rim: 21.5" (54.61 cm)	**Weight:** total wheelchair: 39lbs (17.73kg) rear wheel: 5 lbs (2.27 kg) front castor: 0.8 lbs (0.36 kg)
Tire width: rear: 1.0" (2.54 cm) front: 0.94" (2.39 cm)	**Seat height:** rear: 18.5" (47.00 cm) front: 19.5" (49.53 cm)
Wheelbase: front to back: 16" (40.64 cm) rear: 21.30" (54.10 cm) front: 17.75" (45.09 cm)	**Wheel type:** rear: V, hard rubber front: round, hard rubber
Backrest Height: 17.5" (44.45 cm)	**Percent weight on rear wheels:** 60%

Computers and software

To process and collect the data, various software packages were used on a variety of computers. To collect the data during the experiments a Zenith 286, 16 Mhz processor, was used to run the Grabber2 program that processed the oscilloscope traces. Grabber2 transferred the waveform displayed on the oscilloscope to the computer and created three files: a plot file, an acq file, and an instat file. The plot file generated an oscilloscope screen with the trace on the monitor. The acq and instat files made up the hard data of the waveform that generated a readable waveform preamble

and curve data. These files were converted to an ASCII format file of the waveform for programming purposes.

Digitizing and processing the video tape was on an AST Premium Series 386ST/20 personal computer with the Ariel Performance Analysis System (Ariel Performance Analysis Systems, Inc). This analysis system integrated computer and video processing hardware with specialized software modules that performed data collection, analysis, and presentation. Sequences of images were grabbed off of the video tape and stored on the computer. Each frame was digitized, and the resulting computer sequence was transformed and smoothed. The acceleration, velocity, and distance profiles of the wheelchair were put into ASCII format for the FORTRAN programs.

The various computer programs needed, including the wheelchair model, were developed on the FORTRAN compiler Lahey Personal FORTRAN 77, (B edition, June, 1988). All programming was done on a Zenith 386 personal computer. Microsoft Windows version 3.0 was used to write and edit the programs, which were then linked to the compiler for running.

Analysis of the force profiles was performed using Microsoft Excel version 4.0. This spread sheet allowed the combination of the observed load cell data with the model predicted data, provided the means for statistical analysis and produced the graphs of the profiles.

Calibration of the Load Cell

The calibration of the load cell in tension was executed both statically and dynamically. Static calibration involved hanging weights from the load cell secured to a beam. Dynamic calibration included hanging the weights from the load cell attached to

the Minigym which was suspended from the beam. When the weight was added, the mini gym uncoiled, and the weights dropped to the floor. The signal from the load cell as the weights fell was the desired response. These tests were carried out with combinations of 2 lb, 4.1 lb, and 5 lb weights over the range expected to involve wheelchair propulsion forces: zero to twenty-five pounds (zero to 112 newtons as calculated from power output estimations by Glaser et al., 1980). For each test, a weight was added to the load cell, the response recorded on the oscilloscope, and the data transferred to the computer. Similar conditions and procedures were used for both steps.

Prior to the testing, the zero load baseline signal was set and recorded. To eliminate some error between trials due to a fluctuating baseline, the first horizontal division of each test was left as the zero line. Figure 2 shows the oscilloscope display at the end of the five pound static test demonstrating the baseline and the response to the weight. Each test was accomplished by obtaining a stable zero load signal, adding the designated amount of weight, and saving the response on the oscilloscope. A sweep of 0.5 seconds per division and continuous storage of the trace on the screen allowed enough time to apply the load after the signal was triggered but still leaving a baseline trace at the beginning of each event. The saved screen was then sent to the computer via Grabber2 and stored for analysis.

Both of the static and dynamic calibration data sets were analyzed using the FORTRAN program titled baseline (Appendix A) to convert the absolute grabber numbers to their corresponding value relative to the baseline. This relative value

represents the millivolt change in the signal caused by the weight applied to the load cell. By graphing the weight verses the electrical response, it was shown that the load cell had a linear response to increasing weights. Linear regression gave the least squares fit line.

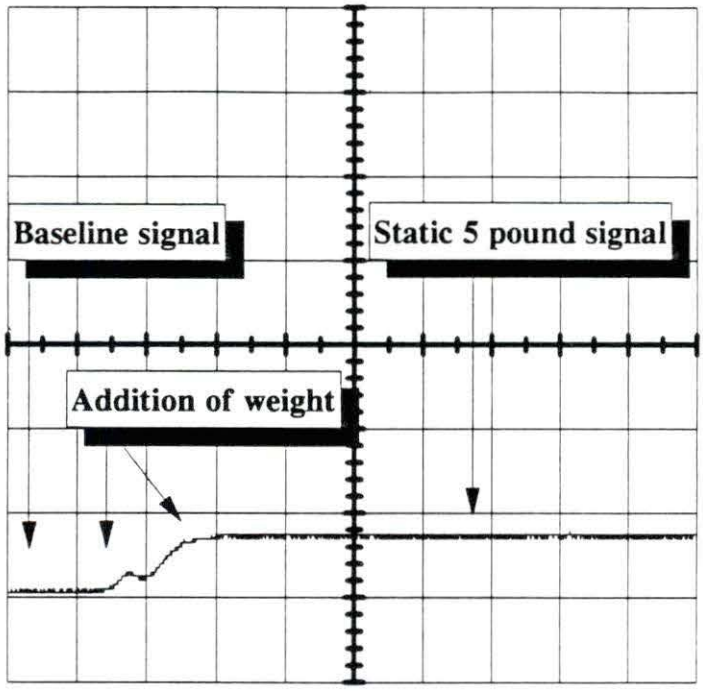

Figure 2. Oscilloscope display of a five pound weight during the static calibration of the load cell

Experimental Procedure

Data collection was composed of two sets of processes performed simultaneously as each subject propelled across the floor. The first set measured the force generated during wheelchair motion while the second set led to the determination of the acceleration and velocity.

The force generated during each test was measured by the load cell which was supported by a sling from the back rest of the wheelchair. The height of the load cell was positioned so that its axes were parallel to the ground and perpendicular to the wheelchair's mid-axle. Standard hex nuts secured two four inch threaded rods (size ½ x 20) to the load cell allowing attachment of the rope. Figure 3 shows the orientation configuration of the load cell as it was used between the Minigym and the wheelchair. The vertical hole at the one end and the horizontal hole at the other allowed integration into the system which maximized freedom of movement of the load cell and reduced unwanted side torques. The load cell was also positioned so that the shielded cable hung down, minimizing twisting and tangling with the Minigym cord.

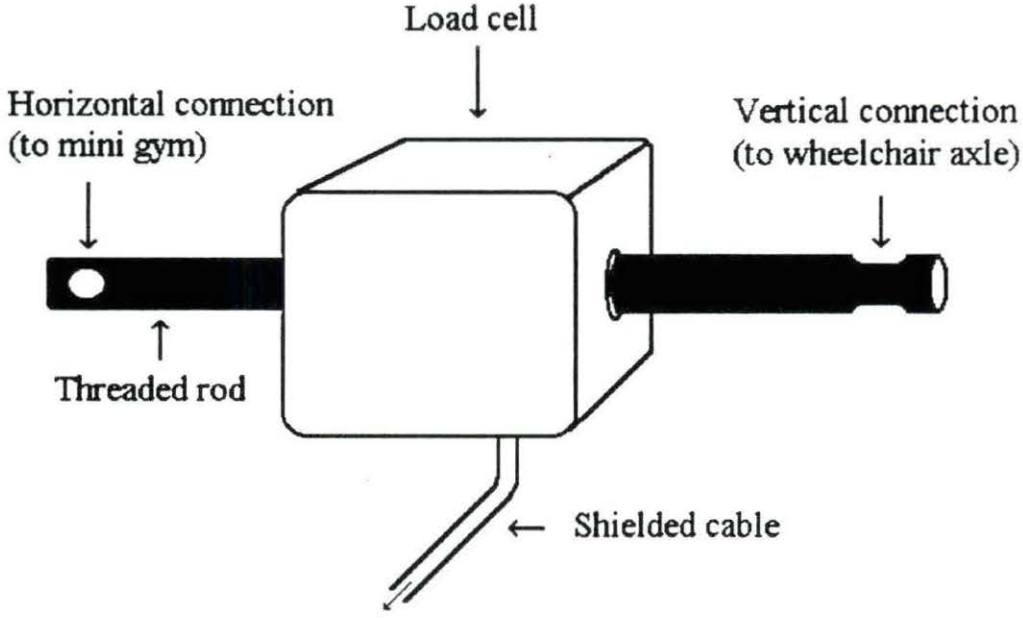

Figure 3. Load cell orientation between the Minigym and the wheelchair

Prior to each trial, the subjects were instructed to pre-load the load cell such that any added force on the push rim caused forward movement. This procedure prevented severe jolting of the load cell and extreme spikes in the data. The pre-loaded values were used as the baseline during analysis as well.

The Minigym was positioned so that the cord was directly in line with the wheelchair axle and the path of the test. Displacement of the Minigym was avoided by securing it to the floor.

The acceleration and velocity of the wheelchair for each test was obtained through digitization of a video tape recording of the event. To aid in digitizing, special reflective markers were placed at numerous points on the wheelchair and subject. The light reflected off of these markers from the spot light was used by the Ariel Performance Analysis System during automatic digitization. The markers were placed on the subject's shoulder, elbow, wrist, the wheelchair's front and rear hub, three locations around the rear wheel spokes, and one on the push bar.

The test area and procedures were established by considering the quality of video recording needed for the digitization process. The camera had to be positioned close enough for a high resolution recording, yet far enough away for the camera to capture a sufficient range of wheelchair motion. As a result, the three phases of motion (starting, constant motion, and stopping) were recorded in segments. Each subject performed nine passes across the field of view of the video camera, three passes for each phase of motion.

The protocol for each segmental test is illustrated in Figure 4. For measuring starts, the subjects were positioned completely in view of the camera to ensure the entire start was recorded. For constant velocity and stopping tests, the subjects started

just outside the camera's field of view enabling them to have extra space for acceleration before recording occurred. In addition, subjects came to a complete stop on or before the completion line only for the stop test. Subjects propelled completely through the field of view for starting and constant motion tests.

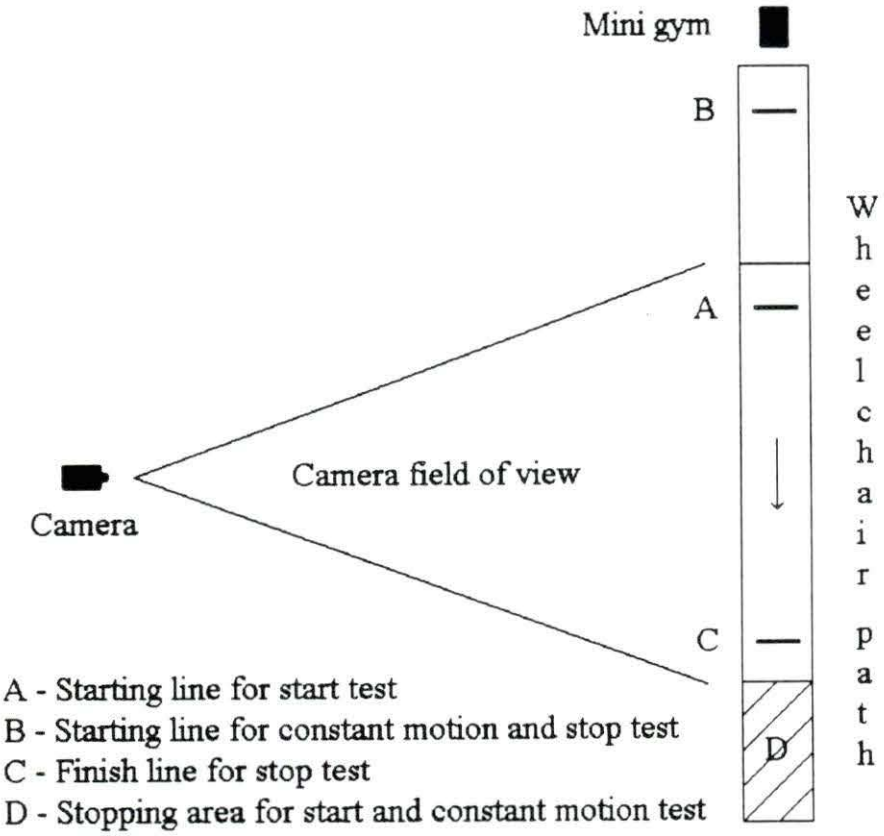

Figure 4. Wheelchair test area: Starting and stopping points

Each subject was given these same instructions concerning where to start and stop for each trial and that attaining fast speeds was not necessary. It was requested that each subject be as consistent as possible for all trials and that several practice runs be taken. Informed consent forms were signed by each subject at the beginning of the

study. Although the order in which the subjects performed the phase tests was randomized, a standard code was used to identify each trial. All starting trials were labeled as 1, 2, and 3, all constant motion trials as 4, 5, and 6, and all stopping trials as 7, 8, and 9. In addition, each subject number preceded the trial number. The code numbers then range from 21 to 89.

Computer Programs

Several FORTRAN programs were written and used for processing the raw data. Also the program that generates the simulation of the wheelchair was written. The codes for these programs are found in Appendix A.

The program "Model" for wheelchair propulsion required the measured dynamic variables and the environmental factors as input, and calculated the force according to the model. A separate file contained dynamic data of each test including the time, distance, velocity, and acceleration profiles of wheelchair movement. The environmental factors are called for during the simulation. The program opened the dynamic data file, read each value and calculated a force for each line of data. All of the input variables, dynamic data, constants and the resulting force calculations are written to an output file for analysis purposes.

Three sets of variables making up the environmental factors were needed for the model. The first set was termed the personal variables and included the mass of the wheelchair and of the user. The computer used these inputs to calculate the normal force of the whole system. The weight distribution of rear to front load was also calculated according to what the user inputs as the distribution ratio. The second set of variables included the wheelchair specifications: the radii of the wheels, castors, and push-rings, and the weight of one rear wheel and one castor. From this input, the

moments of inertia of the two rear wheels and two castors were determined. The third set of variables consisted of the estimates for the drag coefficient, the constant of rolling resistance, and the wheel and castor bearing resistances. Once input for each of these sets of variables was completed, values were stored in a separate file. The program accessed these files during subsequent operations and prompted for reusing the values stored or changing them.

For analysis purposes and to obtain a best fit model, fourteen variations on Cooper's model (Cooper, 1990c) were written using the various alternative models discussed in chapter one. Of the fourteen variations, eight were chosen to be used for statistical analysis because of their accuracy in predicting the observed force. A separate FORTRAN program was written for each variation and force profiles were generated. All programs operated in the same manner as described above. Each trial was evaluated with the eight variations.

In addition to these models, two FORTRAN programs were used to transform the raw observed data into their proper equivalent of force. First of all, the FORTRAN program "Baseline" converted the absolute values to points relative to the established baseline. The program read the baseline section of the input file, systematically subtracted the rest of the file from that data, and produced an output file of the difference. This program was used for both the load cell calibration and the wheelchair data.

Secondly, the FORTRAN program "Force" converted the observed point number to the equivalent force value. The equation used for this process was that of the least squares fit line determined from the calibration of the load cell with the Minigym. Since the load cell was calibrated using pounds of force, this program also converted each value to newtons. In addition, this program subtracted 5.75 pounds

(25.6 Newtons) from each value as a correction factor for the added resistance from the Minigym (see Minigym page 33)

Coordination of Observed and Predicted Data

The coordination of the observed and predicted force profiles of wheelchair motion involved two steps. The first step determined the starting point for each force profile, whereas the second step determined the best beta value to fit the curves. These steps were necessary since the profiles contained excess data, and there was a difference in time measurement between the load cell and the video tape.

For the first step, the starting point for either set of force values was defined as the onset of the first recorded push. Since the load cell measured all of the subject's strokes, a record was kept of which pushes were completely in view of the camera. Separate methods of specifying the exact starting point were used for the observed and predicted force profiles.

For the observed data, since the load cell was pre-loaded prior to each test, the starting point for the starting phase of motion was taken as the first increase from the baseline. For the other two phases of motion, the starting point corresponded to the zero force value just as the first video recorded push was beginning.

For the predicted force profiles, the starting points were determined from evaluations of the distance, velocity, and acceleration profiles prior to using this data in the model programs. From the digitization process, excess data prior to each starting point was acquired ensuring recording the entire event. The initial point for starting phases corresponded to the point where a positive change in distance and velocity began. The beginning of the first recorded push for the other two phases was set at the onset of the corresponding increase in velocity.

For the second step, beta was defined as the time adjusted value needed to account for the time span difference between data sets. A beta value was determined for each trial for all subjects. Time was normalized for both the observed and predicted force profiles. The predicted data time intervals were then multiplied by beta and analysis was done on matching points. A best beta value for each trial was determined by averaging the absolute value difference between the observed and predicted data over the entire time span. The lower this average (called the index value), the better the beta value. The index value was used for statistical analysis and determining the most valid model.

Filtering and Smoothing Techniques

Smoothing the acceleration, velocity and distance data was done using a digital filter with a 3.0 hz cutoff frequency. This frequency was used for two reasons. First, Graeme Wood (1982) used frequencies in this range for gait analysis, an activity attaining speeds similar to that of slow wheelchair propulsion. Secondly, three points on the wheelchair were digitized with the expectation that, without any system error, the accelerations of each of these points should be the same. After smoothing at the frequency of 3.0 hz, the accelerations of each point were similar, yet without sacrificing much data.

Statistical Analysis

Several statistical tools were used to analyze the different categories of data received. For the calibration of the load cell, the linear regression was used utilizing the method of least squares to estimate the best fit line of the weight verses the

numerical response obtained. This procedure was used along with finding the correlation coefficient for both the static and dynamic calibrations.

The closeness of each model's prediction to the observed force was measured by calculating an index value. This index value, as mentioned above, was the average absolute difference between the observed data and the predicted data. Using analysis of variance on these index values over all subjects for each phase of motion led to the determination of a best fit model. In addition, standard t-tests demonstrated the amount of significance difference between models.

RESULTS AND DISCUSSION

The data collected and the statistical analysis of the results from a three step modelling process led to the verification of a model to predict the force required to propel a wheelchair. The first step involved analyzing the results from the calibration of the load cell. These results showed a linear response of the load cell to increasing weights for both static and dynamic calibrations. The second step involved both statistically and visually analyzing the original eight models. Averaging the index values obtained from all subject's trials showed that model two best predicted each phase of motion. Visual analysis of graphs containing the theoretical and the actual forces illustrated that different models had better predictions for different subjects. These observations led to the development for four new models using model two as a base for obtaining one model that best predicted all subjects. The third step involved a similar analysis of this second set of models. Averaging the index values and visually comparing the graphs indicated that a separate model be used for each of the three phases of motion. The following section presents the results obtained from the calibration data and the results for each set of models.

Calibration of the Load Cell

The calibration of the load cell in tension, both statically and dynamically, showed that the electrical response to increasing weights was linear. Regression analysis produced the method of least squares best fit line for each case.

The results of the static calibration are shown in Table 1 and graphically illustrated in Figure 5. The best fit line had a slope equal to 2.69 and had a y intercept at 0.09. The correlation coefficient for this line is $r = 0.999$. This demonstrates that

from r^2, 99.9% of the variation in the response values is accounted for by a linear relationship with the corresponding weight values. The 'Response' values in Table 1 represent the mean displacement of the electrical signal from the baseline as seen on the oscilloscope screen. For each weight, the signal was recorded for one oscilloscope sweep and the response value was averaged over the entire event.

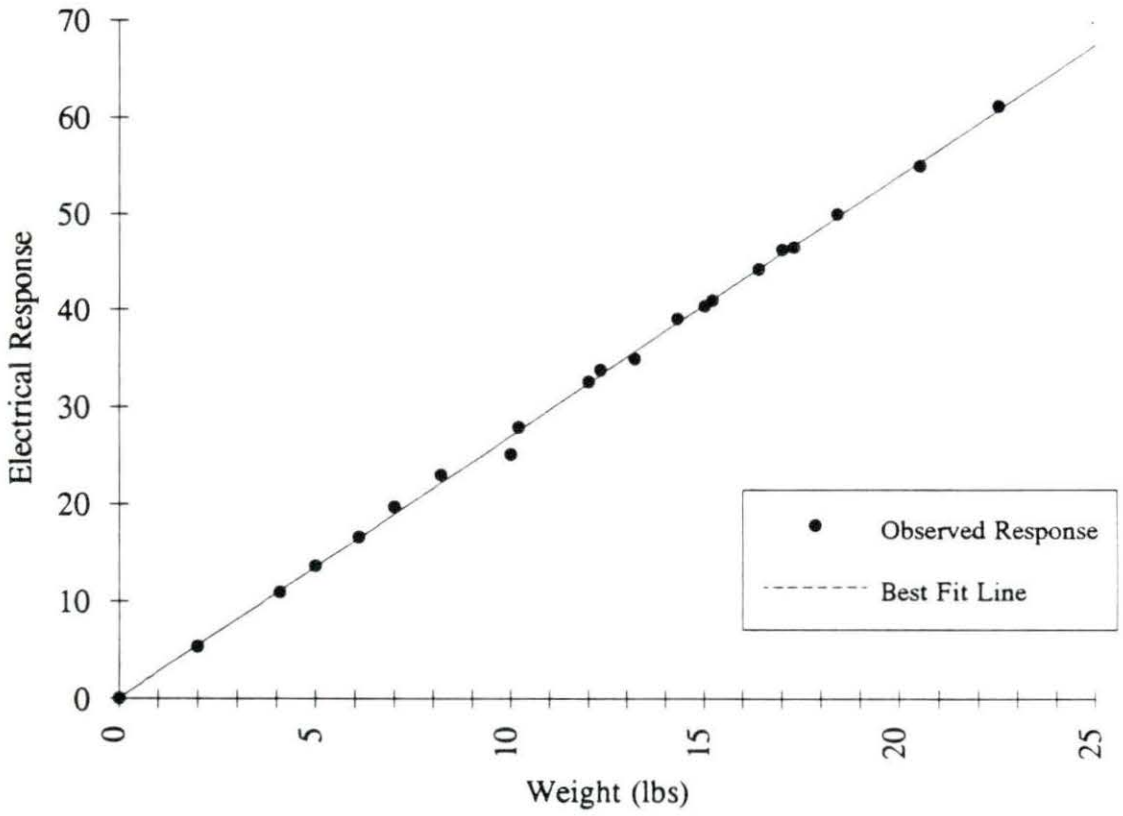

Figure 5. Static calibration of the load cell

Table 3. Static calibration of the load cell

		Weight (lbs)	Response [a]			
	n	(X)	(Y)	X*Y	X^2	Y^2
	1	0.0	0.00	0.00	0.00	0.00
	2	2.0	5.33	10.66	4.00	28.41
	3	4.1	10.96	44.94	16.81	120.12
	4	5.0	13.65	68.25	25.00	186.32
	5	6.1	16.65	101.57	37.21	277.22
	6	7.0	19.64	137.48	49.00	385.73
	7	8.2	22.98	188.44	67.24	528.08
	8	10.0	25.10	251.00	100.00	630.01
	9	10.2	27.85	284.07	104.04	775.62
	10	12.0	32.50	390.00	144.00	1056.25
	11	12.3	33.70	414.51	151.29	1135.69
	12	13.2	34.80	459.36	174.24	1211.04
	13	14.3	38.95	556.99	204.49	1517.10
	14	15.0	40.27	604.05	225.00	1621.67
	15	15.2	40.90	621.68	231.04	1672.81
	16	16.4	44.14	723.90	268.96	1948.34
	17	17.0	46.20	785.40	289.00	2134.44
	18	17.3	46.42	803.07	299.29	2154.82
	19	18.4	49.86	917.42	338.56	2486.02
	20	20.5	54.86	1124.63	420.25	3009.62
	21	22.5	61.00	1372.50	506.25	3721.00
SUM	21	246.70	665.76	9859.90	3655.67	26600.30
		[b] Sxx = 757.53			slope = 2.69	
		Syy = 5493.81			*y* intercept = 0.09	
		Sxy = 2038.81			r = 0.999	

[a] Average numerical response value of the electrical signal from the load cell.

[b] Equations for calculating least squares fit line.

$Sxx = \Sigma x_i^2 - 1/n*(\Sigma x_i)^2$ slope = Sxy/Sxx

$Syy = \Sigma y_i^2 - 1/n*(\Sigma y_i)^2$ *y* intercept = $1/n * [(\Sigma y_i) - \text{slope}*(\Sigma y_i)]$

$Sxy = \Sigma (x_i * y_i) - 1/n*(\Sigma x_i)*(\Sigma y_i)$ $r = Sxy/(Sxx*Syy)^{1/2}$

The results of the dynamic calibration are graphically presented in Figure 6 with the numerical data in Table 2. The best fit line had a slope equal to 2.15 and had a *y* intercept of 3.22. The correlation coefficient, r, for this line is 0.997. From r^2, 99.8% of the variation of the response values was accounted for by a linear relationship with the weight values. The *y* coordinate again represents the average recorded response of the weight. In this case however, the weights and the load cell were allowed to free fall from the minigym. The length of actual response over which the average was taken was limited by the time between when the weights were released and when they hit the ground.

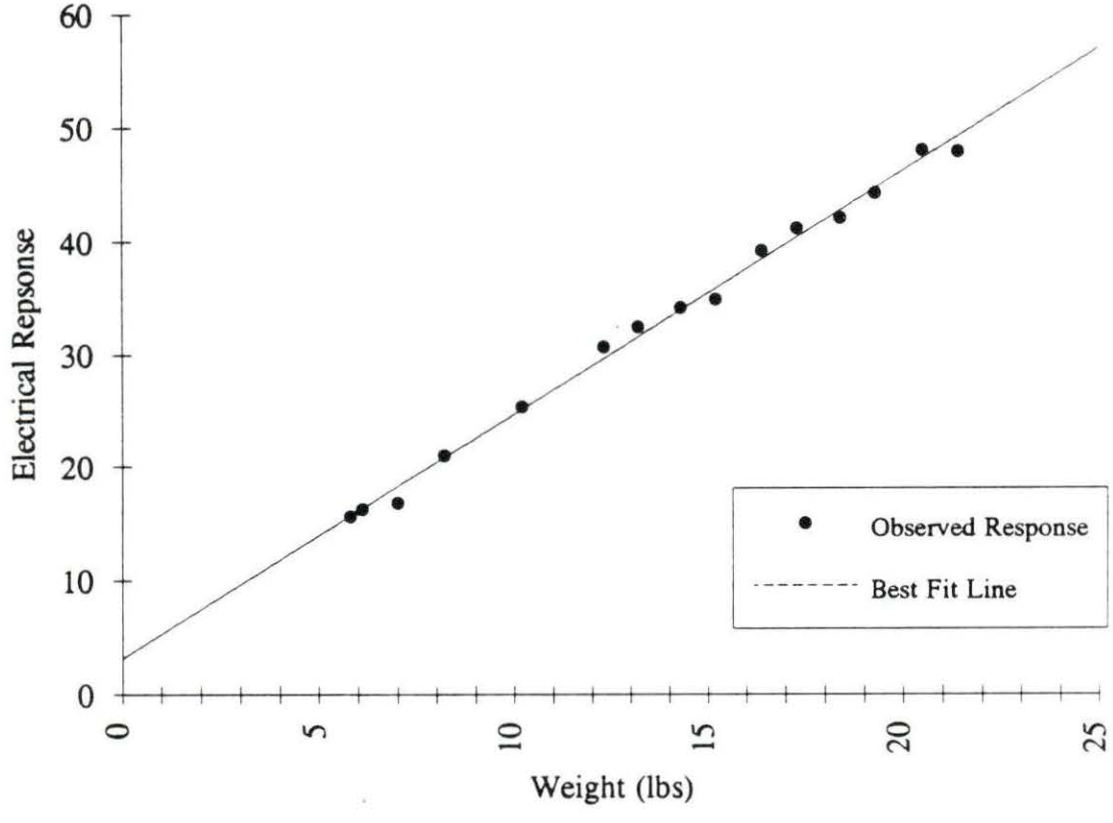

Figure 6. Dynamic calibration of the load cell with the minigym

Table 4. Dynamic calibration of the load cell with the minigym

		Weight (lbs)	Response [a]			
	n	(X)	(Y)	X*Y	X^2	Y^2
	1	5.8	15.60	89.86	33.18	243.36
	2	6.1	16.25	99.13	37.21	264.06
	3	7.0	16.77	117.39	49.00	281.23
	4	8.2	21.01	172.28	67.24	441.42
	5	10.2	25.34	258.47	104.04	642.12
	6	12.3	30.66	377.12	151.29	940.04
	7	13.2	32.42	427.94	174.24	1051.06
	8	14.3	34.14	488.20	204.49	1165.54
	9	15.2	34.87	530.02	231.04	1215.92
	10	16.4	39.15	642.06	268.96	1532.72
	11	17.3	41.17	712.24	299.29	1694.97
	12	18.4	42.07	774.09	338.56	1769.89
	13	19.3	44.23	853.64	372.49	1956.29
	14	20.5	47.98	983.59	420.25	2302.08
	15	21.4	47.87	1024.42	457.96	2291.54
SUM	15	205.6	489.53	7550.45	3209.24	17792.23
		[b] Sxx = 392.25			slope = 2.15	
		Syy = 1816.26			y - intercept = 3.22	
		Sxy = 841.93			r = 0.997	

[a] Average numerical response value of the electrical signal from the load cell.

[b] Equations for calculating least squares fit line.

$Sxx = \Sigma x_i^2 - 1/n*(\Sigma x_i)^2$ slope = Sxy/Sxx

$Syy = \Sigma y_i^2 - 1/n*(\Sigma y_i)^2$ y intercept = $1/n * [(\Sigma y_i) - \text{slope}*(\Sigma y_i)]$

$Sxy = \Sigma (x_i * y_i) - 1/n*(\Sigma x_i)*(\Sigma y_i)$ $r = Sxy/(Sxx*Syy)^{1/2}$

The Minigym resisted movement; it was experimentally determined that a minimum of 5.8 pounds would be needed to initiate and maintain motion. Measurements involved several trials in which a maximum force was applied in tension with the load such that the minigym did not uncoil. The average of these trials resulted in a maximum static response of 15.60. Using the best fit line for static calibration, the corresponding force was 5.8 pounds. This value was estimated mathematically by finding the point of intersection of the two best fit lines. The x coordinate for this point was 5.79, yielding a 0.17% error. These calculations rely on the exact setting of the minigym resistance, which remained unchanged for the duration of the experiment.

Estimation of the Beta Value

As shown in Figure 7, there was a phase shift due to a time measurement difference between the load cell observed data and the model predicted data. This lag is considered to be a result of a recording error involved in filming with a video camera. Although the camera specifications indicate that filming speed is thirty frames per second, fluctuations from this rate occur. Various factors of normal operations including power surges, repeatedly turning on and off the recorder, and the changing length of tape on the spools contribute to the fluctuations. The error in time estimation then surfaced when the digitization process was based on a strict 30 frames per second interval.

To adjust for this time lag, the time scales for both the observed and theoretical profiles were normalized and an initial first guess for beta was first estimated by averaging quotients of respective critical points of the data set. A point in time for an observed maximum was divided by the corresponding time for a predicted maximum. Points A and B in Figure 7 demonstrate examples of the critical points used. The

average over several points provided the best guess for the beta value. This initial guess proved to be the best beta value for 75% of the trials based on the lowest index value as the method of measure. Figure 8 shows the results of the horizontal adjusted from the application of beta to subject KH trial 3.

Analysis of the beta values with the length of time for the event showed a correlation coefficient of 0.222 indicating very little connection between the two variables. As a result, the best estimate of beta is the mean. For all trials the mean beta value was 1.15 with a standard deviation of 0.093. Table 5 shows the beta values used for each trial of each subject. The mean length of time for each trial was 2.22 seconds with a standard deviation of 0.42.

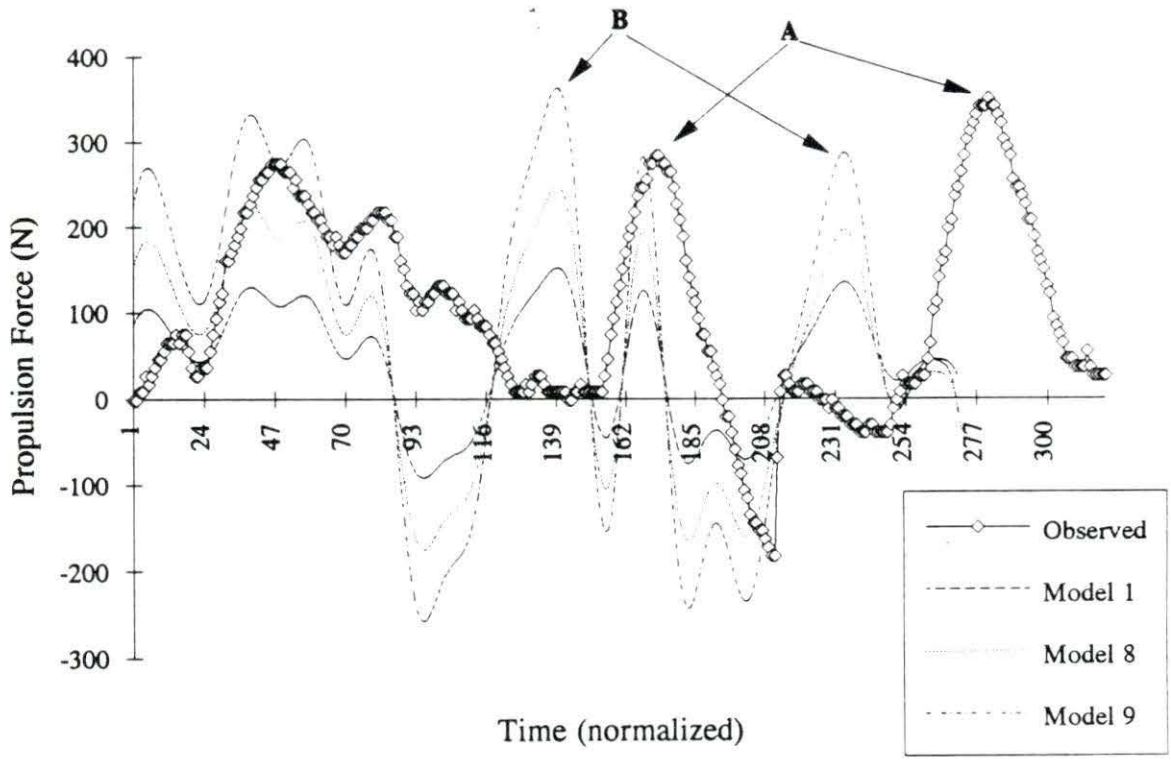

Figure 7. Time lag between observed and predicted force profiles for subject KH trial 3 **A** refers to two critical points of observed data and **B** refers to the two corresponding points of the theoretical data

Table 5. Beta adjusted values for each subject and trial

Subject	Trial 1	Trial 2	Trial 3	Trial 4	Trial 5	Trial 6	Trial 7	Trial 8	Trial 9
KH	1.00	1.25	1.21	1.20	1.17	1.24	1.21	1.30	1.10
GN	1.20	1.08	1.14	1.20	1.12	1.00	1.24	1.30	1.30
VD	1.16	1.17	1.13	1.17	1.20	1.08	1.05	1.30	1.25
SK	1.08	1.16	1.13	1.23	1.00	1.04	1.25	1.30	1.23
BF	1.00	1.17	1.19	1.10	1.05	1.00	1.30	1.00	0.90
CO	1.16	1.14	1.17	1.08	1.20	1.09	1.21	1.21	1.04
RK	1.14	1.07	1.09	1.19	1.10	1.20	1.10	1.20	1.01
		Sum X = 72.30			Mean = 1.15				
		Sum X^2 = 83.51			Standard Deviation = 0.09				

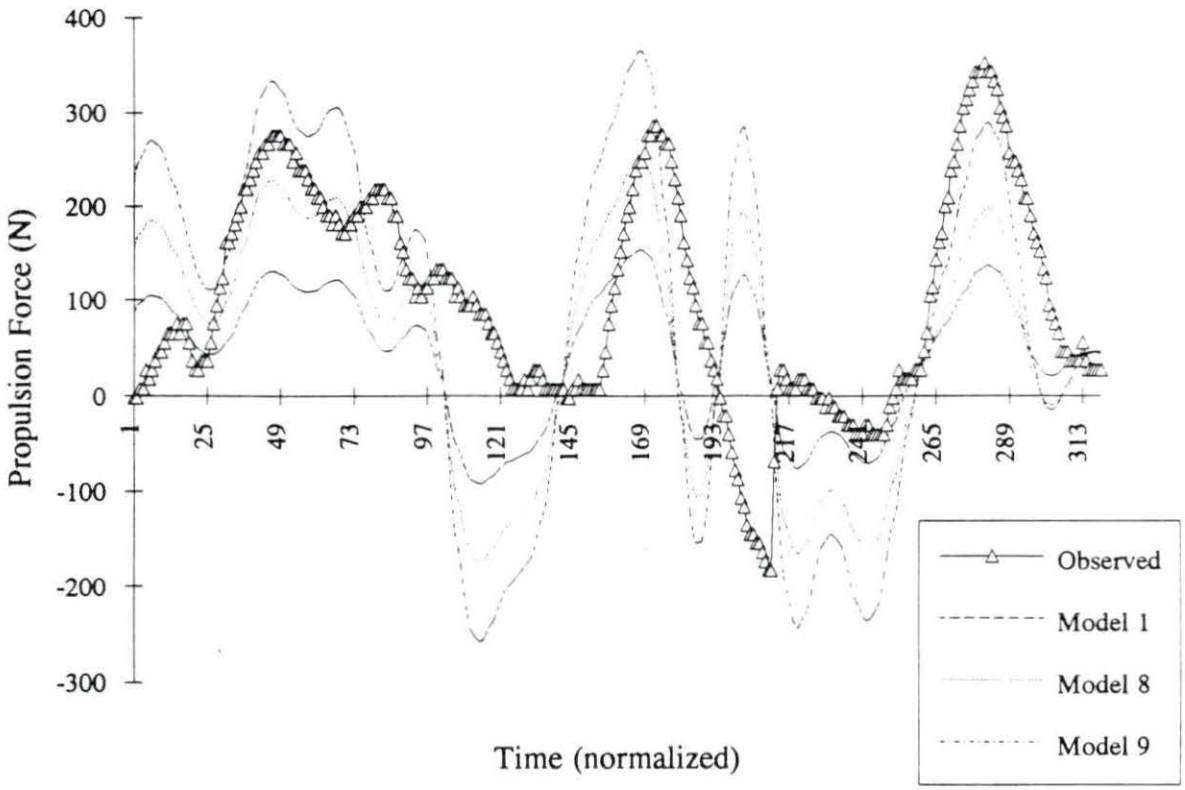

Figure 8. Time lag adjustment for theoretical force profiles using a beta value of 1.21 for subject KH trial 3

Propulsion Mechanics

Evaluating the observed and the predicted forces was done both on an individual trial basis and on an average phase basis. In Figure 8, each of the three major peaks from the observed profile represents one stroke or push on the hand rim by the subject. Each subject had three strokes recorded per trial except for a few cases in which there was only two strokes.

The observed forces received were found to compare favorably with results reported in literature. Although no results of force changes over time during propulsion have been published, power output, defined as the product of force and

velocity, has been studied using standard wheelchairs. Samuelsson et al. (1991) reported that the maximum power output encountered for wheelchair velocities between 0.64 and 1.60 m/s ranged from 228 to 465 watts. For comparison purposes, the peak force for each stroke was averaged within a trial and multiplied by the average velocity. The results for each phase are shown in Table 6 and the cumulative results are graphically presented in Figure 9. The relationship between the velocity and peak power output for the cumulative results had an overall correlation coefficient of 0.89. The method of least squares gave $y = 438.5 * x - 171.6$ as the best fit line. In addition, Table 6 shows the best fit line for each phase with the corresponding correlation coefficient. Comparison to other data commonly found in the literature such as power output verses weight or average force verses weight cannot be made since neither the force load nor the velocity of the subjects were controlled.

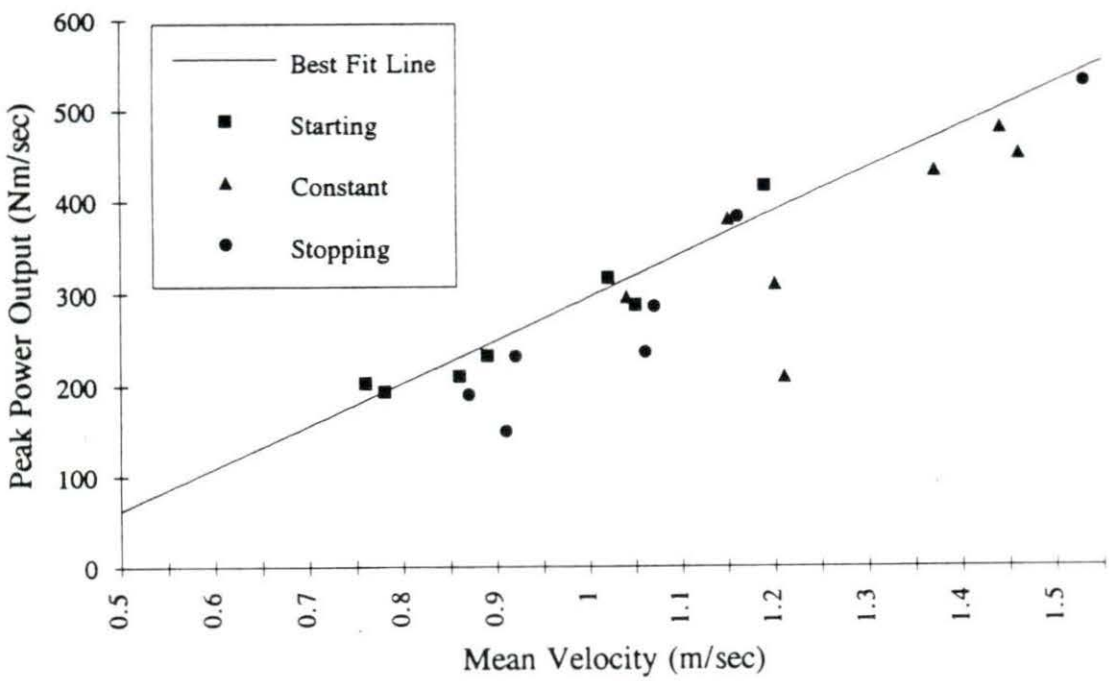

Figure 9. Relationship between peak power output and velocity for each phase of motion and subject

Table 6. Mean peak force, velocity and power output for each phase of motion

Subject	Phase of Motion	Mean Peak Force (N)	Mean Velocity (m/sec)	Power Output (Nm/sec)
KH	Starting	268.77	0.76	202.91
	Constant	260.27	1.20	311.09
	Stopping	163.74	0.91	149.55
GN	Starting	245.43	0.86	210.63
	Constant	284.70	1.04	296.82
	Stopping	254.43	0.91	232.49
VD	Starting	247.55	0.78	193.67
	Constant	174.36	1.20	209.43
	Stopping	217.83	0.87	190.14
SK	Starting	261.33	0.89	232.91
	Constant	330.28	1.15	381.20
	Stopping	266.64	1.07	286.37
BF	Starting	349.10	1.19	416.77
	Constant	334.90	1.44	481.63
	Stopping	223.72	1.06	236.48
CO	Starting	276.19	1.04	287.58
	Constant	310.66	1.46	452.81
	Stopping	346.74	1.53	531.83
RK	Starting	311.20	1.02	317.42
	Constant	315.43	1.37	433.52
	Stopping	333.99	1.15	383.59

Method of least squares best fit lines

Phase	Slope	Y intercept	Correlation Coefficient
Starting	495.2	-196.8	0.97
Constant	478.6	-239.3	0.77
Stopping	552.8	-306.2	0.96
Overall	468.4	-171.6	0.89

To determine how each subject responded to the testing of the different phases of motion, an average acceleration for each phase was calculated. These results are found in Table 7 and indicate that a distinction can be made between phases. In all subjects the average acceleration for starting was positive and larger than in the other phases whereas acceleration was closer to zero for constant motion. Most subjects also showed an overall negative acceleration for the stopping phase. However, the digitized film records for subject CO indicate that he did not come to a complete stop within the test region which explains why his mean stopping acceleration is greater than zero.

Table 7. Mean accelerations (m/sec^2) for each phase of motion

Subject	Starting	Constant	Stopping
KH	0.34	0.09	-0.21
GN	0.27	-0.02	-0.50
VD	0.24	-0.12	-0.60
SK	0.29	0.02	-0.40
BF	0.71	0.21	-0.50
CO	0.79	0.39	0.04
RK	0.59	0.23	-0.28

Initial Model Development

The establishment of the fourteen variations of the wheelchair model was based on the different methods of modeling as described in the literature review and used for statistical analysis purposes. The variations generated (Appendix A) are varied by the inclusion or exclusion of a term, and/or by a different mathematical representation of a parameter. The air drag term, for example, was varied by the two methods of predicting it (Coe, 1979; and McLaurin and Brubaker, 1991) and whether the term was needed in the equation at all.

Preliminary studies of the fourteen model variations reduced the number to a possible eight that had potential of being valid force predictors. There were two reasons for an initial elimination of a model variation. The first reason was that its force prediction did not come close to the observed profiles. The second reason was that there was a lack of difference between two or more models. Being close was defined as having the index value difference between two models to be less than 5%. Models one through four and thirteen were set up to test the significance of the air drag and bearing resistance terms. The rest of the variations were then grouped according to their closeness. In these additional groups, only one model was chosen if the difference was a result of a variation of the air drag or bearing resistance.

Model Analysis

Statistical analysis of the eight models demonstrated the significant difference between and within the groups based on the trial and phase index values obtained. Tables 8, 9, and 10 show the groups of models obtained with the mean trial index calculated from all subjects over the given phase of motion. Models within the same group are not significantly different and are ranked from high to low according to their

mean index value. Models with the lowest index value were considered the best predictors. The level of significance was established by a least significance difference t test for the variable index. The mean phase index as shown in Tables 8, 9, and 10 was obtained after the time lag adjustment by averaging the three trials of each phase of motion for each subject. Averaging the phase index values over all subjects then represents the mean phase index. All mean trial and mean phase index values can be found in Appendix C.

Table 8. Model groups of significance with the mean trial index and the mean phase index for the starting phase of motion

Starting Phase			
Group	Model	Mean Trial Index	Mean Phase Index
A	9	177.23	146.97
B	10	120.90	98.68
	8	128.77	98.46
C	13	103.92	86.13
	4	103.94	85.66
	1	103.57	85.26
	3	102.79	84.10
	2	102.19	83.38

Table 9. Model groups of significance with the mean trial index and the mean phase index for the constant propulsion phase of motion

Constant Motion Phase			
Group	Model	Mean Phase Index	Mean Phase Trial
A	9	178.94	135.46
B	10	125.39	95.00
	8	125.24	94.87
C	13	106.82	86.91
	1	106.75	87.07
	4	106.68	86.86
	3	105.25	84.25
	2	105.22	84.45

Table 10. Model groups of significance with the mean trial index and the mean phase index for the stopping phase of motion

Stopping Phase			
Group	Model	Mean Trial Index	Mean Phase Index
A	9	194.76	160.90
B	10	126.89	95.84
	8	126.60	95.41
C	13	101.33	86.63
	1	101.28	86.70
	4	100.27	84.87
	3	97.22	80.04
	2	97.18	80.10

As demonstrated in Tables 8, 9, and 10, model two is the best predictor of the observed forces for each phase of motion according to the mean trial index. Recall that the models in group C all have the same acceleration and rolling resistance terms and are varied by the bearing resistance and air drag terms. Group C models having no significant difference (their difference can be attributed to error) demonstrates that the air drag and bearing resistance terms do not play a significant role in the prediction of standard wheelchair propulsion. The inclusion of these terms neither added nor subtracted from the overall force prediction. Although the mean phase index indicated that model three was the best predictor for constant motion and stopping phases, there was essentially no difference between model two and three. Since the model groups were the same for both sets of indexes, the mean phase index was included for comparison reasons.

The difference between groups of models was accounted for by a combination of changes in the rolling resistance and mass acceleration terms. Models eight, nine, and ten used a method of predicting rolling resistance as derived by LeMaire et al. (1991) and did not contain the moments of inertia constants in the mass acceleration term.

The exclusion of the inertia terms was also a result of no significant difference with models that included it. Model six, although not included in the final analysis, was used for four subjects as it was mathematically similar to model nine except that it had no inertial terms of the front and rear wheels. Analysis of the mean index value over the subjects used showed no significant difference with the mean index value of model nine averaged over the same subjects. This was true for each phase of motion. With this in mind, the difference between groups can therefore be accounted for by the rolling resistance term used.

For insight into the importance of the rolling resistance term, the graphical comparisons of each trial were studied along with the individual index values. Visual analysis of the graphs involved comparing the maximum force prediction with what was observed. As can be seen in Figure 10, group A models predict a higher force than group B or group C. This trend was true for all subjects and all trials. In addition, Figure 10 also demonstrates that for this particular trial, model group B was the best predictor in terms of a positive force magnitude. This sort of visual analysis along with the index values led to the following three observations and the second group of models. For simplification purposes of the following graphs, models two, eight and nine serve as the representative for their respective significance groups.

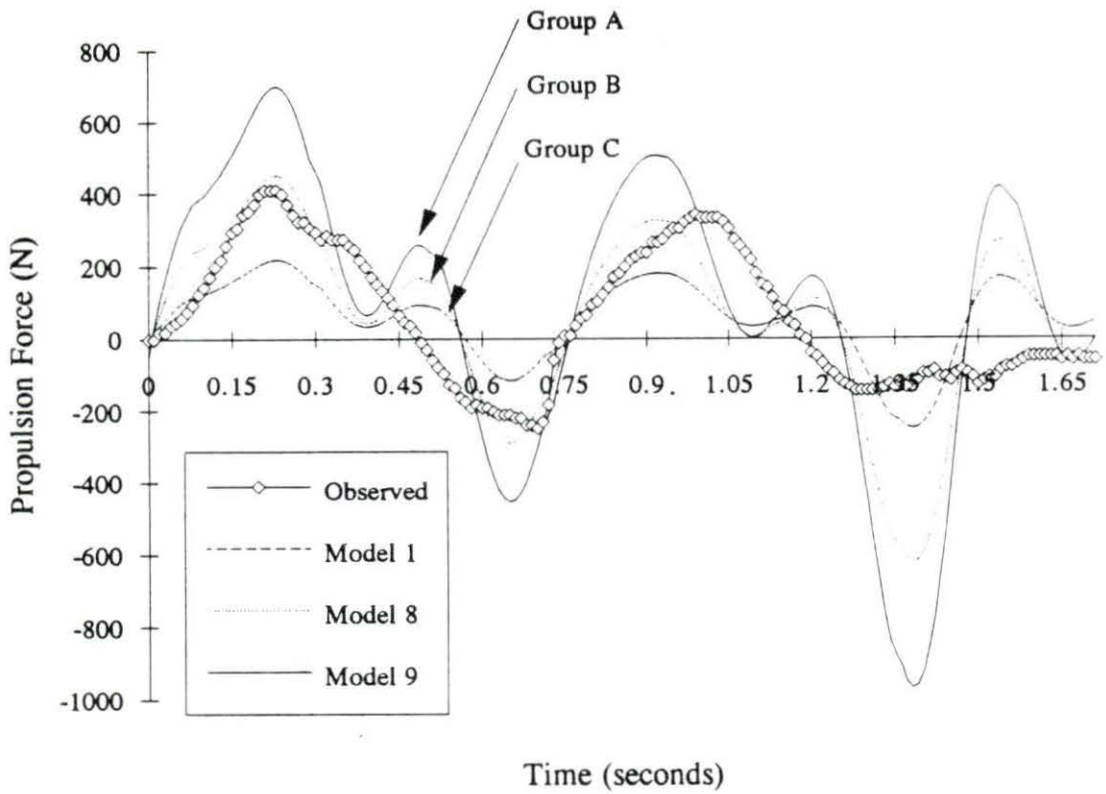

Figure 10. Model groups of comparison for subject BF trial 5 **Index values:** Model 2 - 113.75; model 8 - 128.35; model 9 - 218.27

The first observation was that the model with the best positive amplitude prediction did not always have the lowest index value. As shown in Figure 11, the magnitude of the force for each stoke was most accurately predicted by model nine. However, the lowest index value obtained for this trial was 79.8 produced by model two. Model nine had an index value of 119.8. From Figure 11, model two is clearly not the best model predictor. This discrepancy can be explained mathematically by observing that the models that displayed higher forces also have larger negative forces. With the index based on the absolute value difference between the profiles, the large negative values increased the average index. This trend followed for subjects whose peaks were best predicted by group A and B models for constant motion and stopping phases. In the starting phase, the subjects attempted to accelerate continuously and thus avoided the large decelerations between stokes. In these cases, the model that predicted best visually generally had the lowest index.

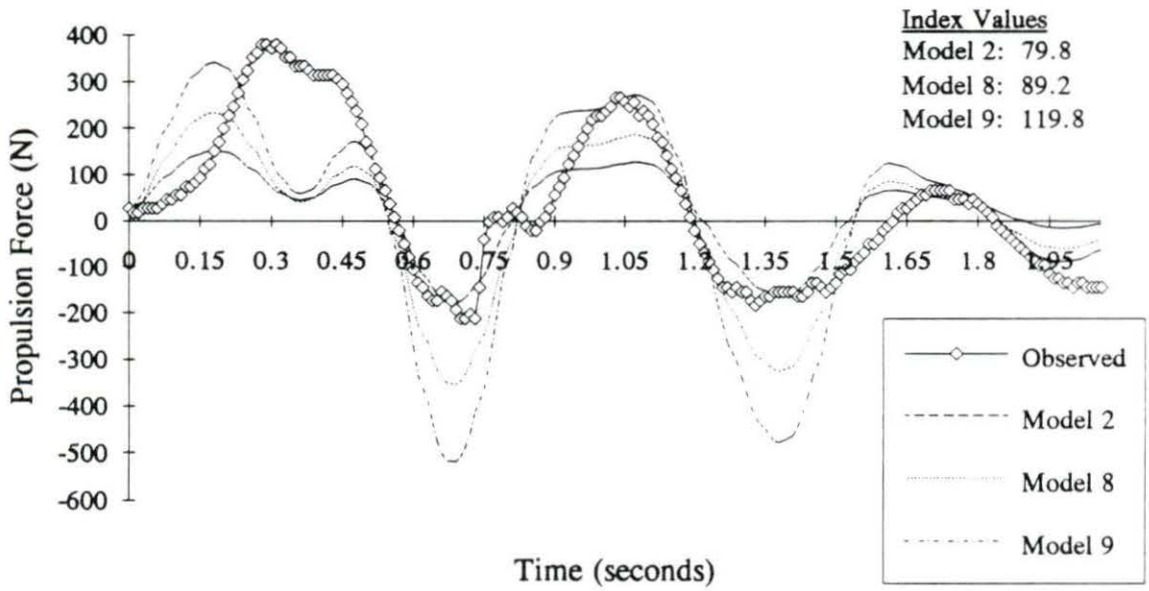

Figure 11. Profile for subject VD trial 5 showing discrepancy between best amplitude predictor and lowest index value

The second observation was that the best model predictor of force magnitude varied within a subject trial. As can be seen in Figure 12, the first peak identifies best with model nine, the second peak with model two, and the third peak with model eight. When the observed forces show changes in magnitude from one peak to the next, the theoretical profiles do not always reciprocate. In Figure 12 the observed force shows a decrease in magnitude from stroke one to stroke two, whereas all model groups show an increase. Even though this observation was found in all subjects and in each phase of motion, peak to peak changes were predicted accurately in approximately equal number of trials. The results of the second set of models will later demonstrate some conclusions that can be drawn on this seemingly random occurrence.

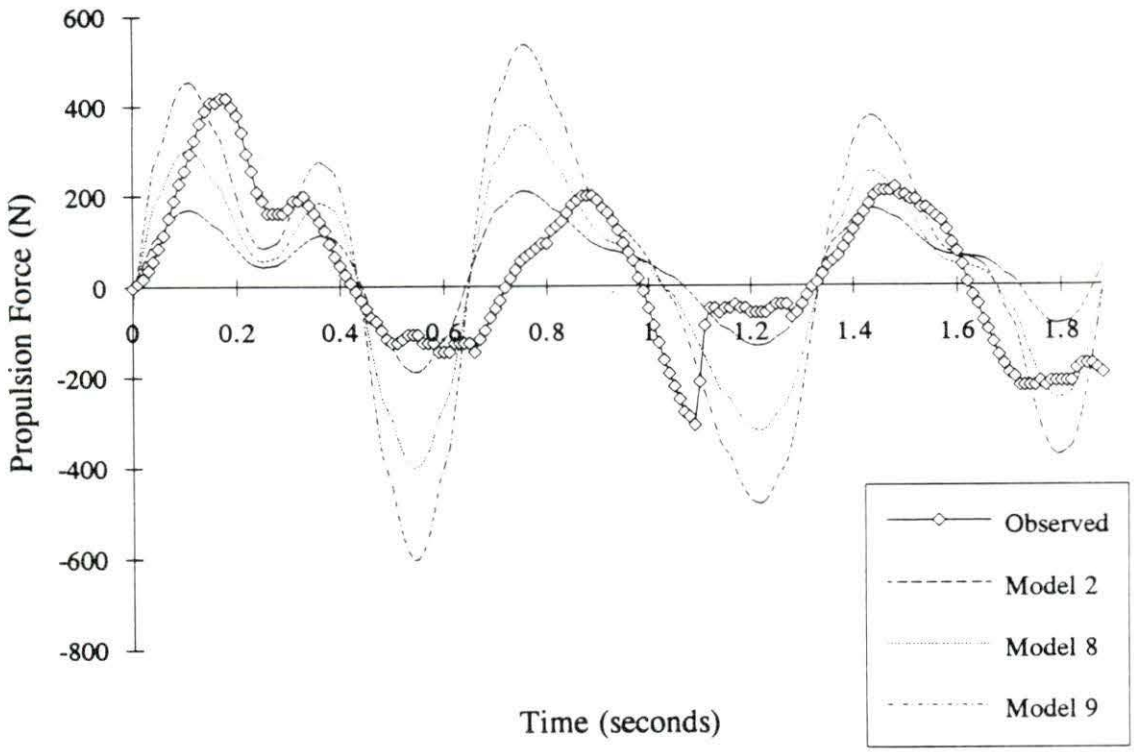

Figure 12. Force profiles depicting various model groups predicting the different peak forces for subject RK trial 7 **Index values:** Model 2 - 96.79; model 8 - 119.03; model 9 - 174.91

The third observation was that lighter subjects had a different model group as a best predictor in terms of force amplitude than heavier subjects. Although this trend was seen in all phases of motion, it was most evident in the starting phase. Figure 13 demonstrates that for a light subject, model nine most accurately predicts the force magnitudes. On the other hand, for a heavy subject model two best predicts the forces as shown in Figure 14. Trends show that the extreme light and heavy subjects have observed forces that are predicted fairly consistently by the same group of models within a phase. However, subjects who had average weights showed more fluctuations amongst the three model groups as to which model best predicted the observed forces in terms of both the lowest index value and visual comparison. This led to the conclusion that the mass of the subject plays a significant role in the models.

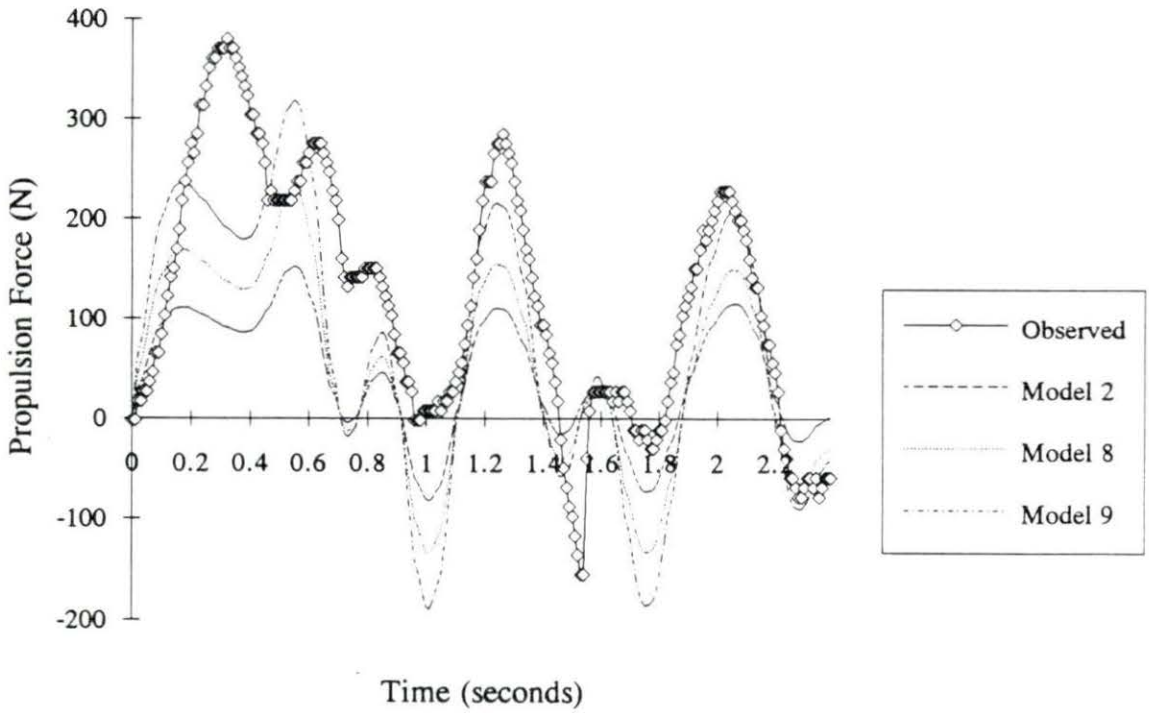

Figure 13. The lightest subject SK has model 9 as a best amplitude predictor for trial 2
Index values: Model 2 - 93.24; model 8 - 84.36; model 9 - 77.40

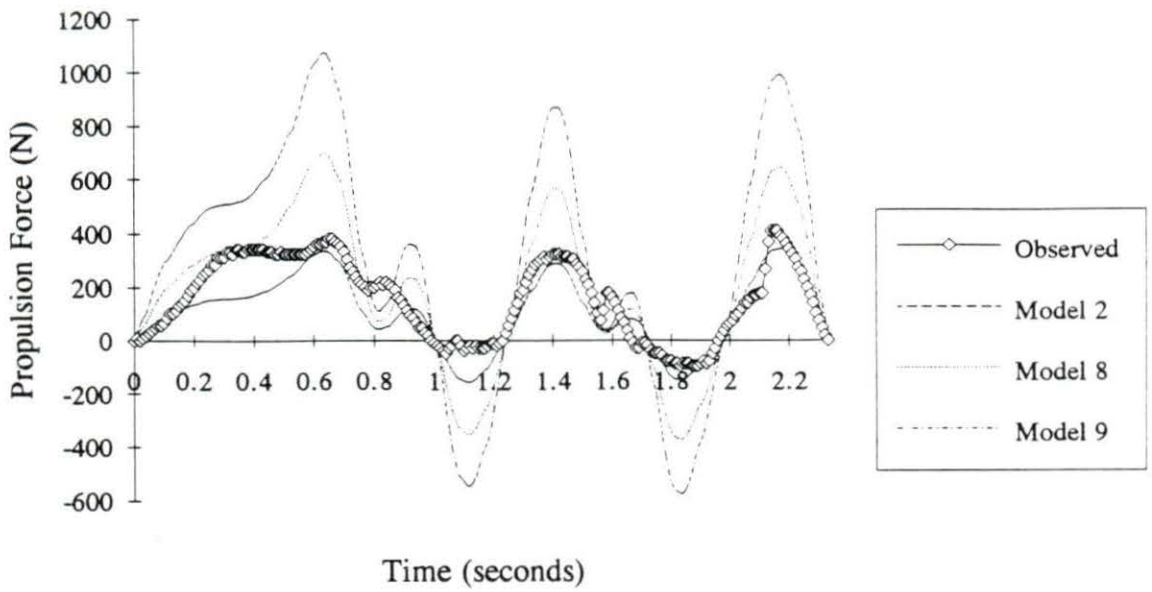

Figure 14. Subject, CO has model 2 as a best predictor of amplitude for trial 2
Index values: Model 2 - 60.93; model 8 - 133.03; model 9 - 282.26

Establishment of the Second Set of Models

The establishment of the second set of models was based on the fact that model two had the best results in terms of the lowest index, but did not accurately predict the force amplitudes for all subjects. The approach taken to improving the model two was established from the three observations as described above. The new model had to account for all subject weights, control the negative swing of the force predictions, and match the changes in maximum forces from stroke to stroke. This task was achieved by establishing an alpha term developed as a function of subject mass. Alpha was used as a linear proportionality constant as it was multiplied by model two. To help control the negative swing, alpha was applied only when the acceleration of the wheelchair was positive. When acceleration was negative, model two was left unchanged. To account

for the differences in peak force predictions, three alphas of increasing magnitude were used and tested. In addition, a fourth model was developed to test the importance of controlling the negative swing.

The four models generated took the form of model two multiplied by a different alpha. The alpha constant was generated in each case from the equation

$$\alpha = (x - W*y)$$

where W is the weight of the subject/wheelchair system. Values for x and y were derived from a sequence of two equations based on different magnitudes of alpha needed. The two extreme subject weights were used for the initial conditions of W in the calculations. Model 21 was derived from:

$$(x - 115*y) = 1$$
$$(x - 70*y) = 2$$

Solving for the two unknowns yielded $x = 3.556$ and $y = 0.0222$. Subject weights between the initial conditions then had an alpha that increased linearly between 1 and 2 for heavy to light subjects respectively.

Model 21 was the model used to see how much effect alpha had during deceleration of the wheelchair. In this model, alpha was exactly the same as in model 22 except that it was also applied while the acceleration values were less than zero. Models 23 and 24 used α's that increased linearly from 1 to 2.5 and 1 to 3.0 respectively. Table 11 gives the values for α, x, and y for all four models.

Table 11. Values for α as calculated from x and y for the second set of models

Model	α	x	y
21 [a]	$1 < \alpha < 2$	3.556	0.0222
22	$1 < \alpha < 2$	3.556	0.0222
23	$1 < \alpha < 2.5$	4.833	0.0333
24	$1 < \alpha < 3$	6.111	0.0444

[a] Model 21 differs from model 22 in that α is applied for the whole profile, not just for positive acceleration.

Analysis of the Second Set of Models

Analysis of the alpha adjusted models proceeded in the same manner as the first set of original models. In this case however, the data from four subjects was chosen to establish the mean trial and mean phase indexes for determining a best model. The four subjects, SK, VD, RK, and BF, were used because their weights ranged from light to heavy. It was found that a different model was needed to predict each of the three phases of motion. Tables 12, 13, and 14 show the mean trial and mean phase index values for the corresponding phase. These models are ranked from high index to low and grouped according to the significance level of $\alpha = 0.05$. The best model for each phase was then used on the other three subject's data to study their validity.

Table 12. Mean trial and mean phase index values for the starting phase of motion for the second set of models

Starting Phase					
Group	Model	Mean Trial Index	Group	Model	Mean Phase Index
A	21	96.41	A	21	73.82
B	24	93.18		22	70.83
	22	92.47		23	67.60
	23	90.33		24	67.25

Table 13. Mean trial and mean phase index values for the constant velocity phase of motion for the second set of models

Constant Motion					
Group	Model	Mean Trial Index	Group	Model	Mean Phase Index
A	24	124.14	A	24	93.94
	21	118.63		23	90.14
	23	117.88		22	88.31
	22	114.21		21	85.94

Table 14. Mean trial and mean phase index values for the stopping phase of motion for the second set of models

Stopping					
Group	Model	Mean Trial Index	Group	Model	Mean Phase Index
A	24	114.31	A	24	99.91
	23	110.17		23	96.82
B	22	107.34		22	94.40
	21	104.56	B	21	84.44

The results obtained for the starting phase indicated that a large alpha was needed to increase the magnitude of the model predictions. From a mechanical point of view, the subject must overcome static friction as well as produce large accelerations. Although the mean phase index shows model 24 to be the best predictor, there is no significant difference between its index and model 23. Studying the graphs confirmed a much improved amplitude prediction over the first set of models for all subjects (see Figure 15).

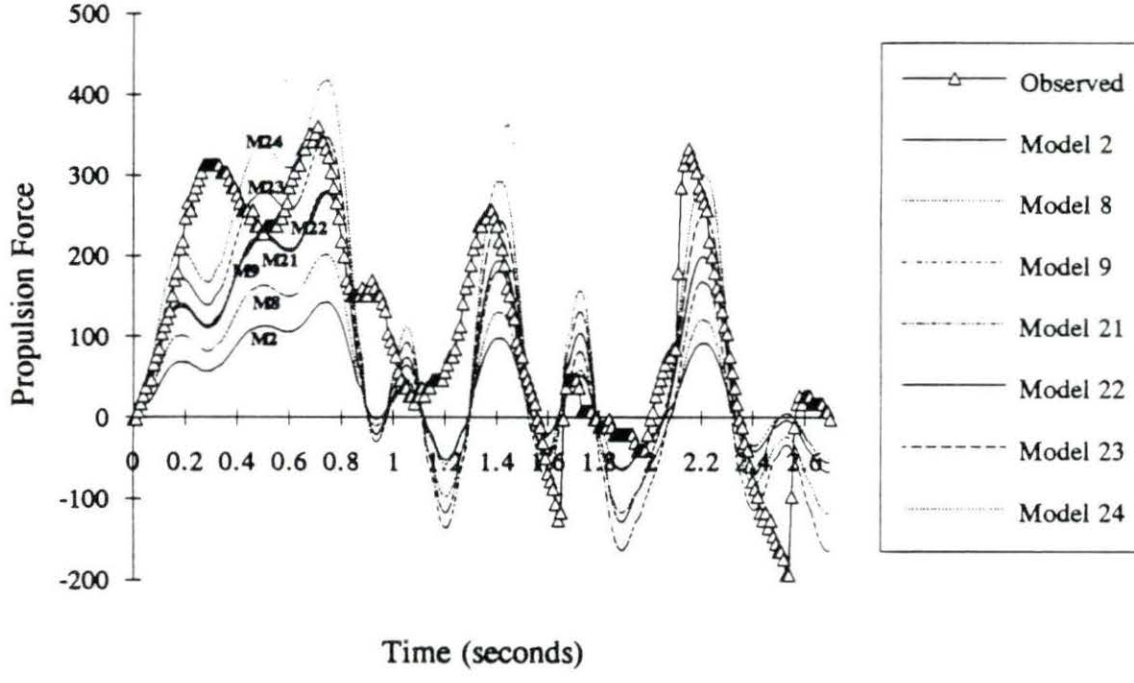

Figure 15. Improved model predictions for the starting phase of motion for subject SK trial 1 **Index values:** Model 2 - 102.03; model 8 - 95.74; model 9 - 83.14; model 21 - 72.99; model 22 - 67.70; model 23 - 61.22; model 24 - 66.77

For constant motion, there was again a discrepancy between the analysis procedures giving the best model predictors as shown in Table 13. There was no significance to this difference. The lack of significance can be explained by the fact that subjects were not perfectly consistent in their propulsion leaving a different model to best predict a peak force. Visually comparing the profiles showed that when the observed peak forces stayed constant within a trial, so did the theoretical profile. Figure 16 demonstrates that model 22 does stay even with the actual force and is an improvement over the original models.

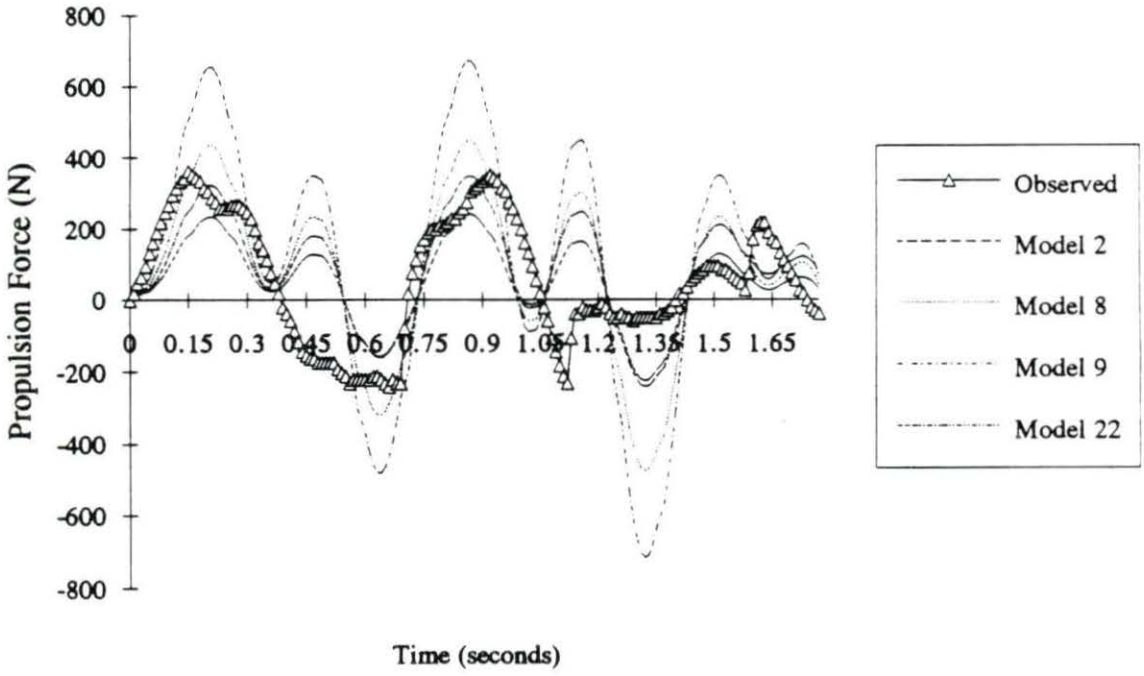

Figure 16. Improvements made by model 22 over the original models for subject RK trial 5 **Index values:** Model 2 - 117.03; model 8 - 145.75; model 9 - 222.59; model 22 - 116.11

Analysis of the stopping phase index values showed that model 21 was the best predictor (see Table 14). This was not surprising since subjects entered the recording area with constant propulsion and then were required to stop. Visual analysis of the propulsion section of these profiles showed they were similar to the constant motion phase. The measurement of stopping showed the observed profile losing force and dropping below the pre-loaded zero line as forward motion stopped. The tension force in the load cell eventually drops back down to the zero load baseline. Since model 21 also increased the magnitude of the deceleration force, it showed both a statistically and visually better prediction than model 22 (see Figure 17).

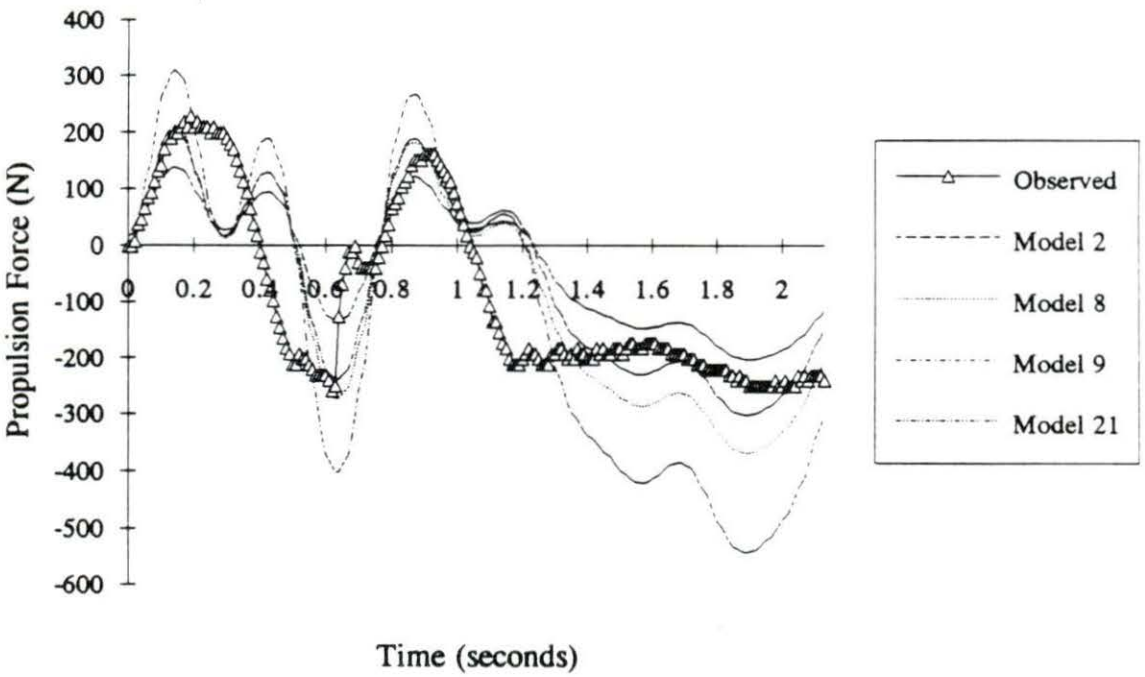

Figure 17. Model 21 improvements for the stopping phase of subject VD trial 9 **Index values:** Model 2 - 85.95; model 8 - 87.25; model 9 - 152.73; model 21 - 73.96

Application of Best Models

To test the validity of the second set of models, the best predictors were applied to their respective trials of the three remaining subject's data. These subjects, KH, GN, and CO similarly represented the range of weights involved in the experiment. In addition, the mean beta adjustment value of 1.15 was used to test its use as the best time adjuster. Table 15 gives the mean trial and the mean phase indexes for each phase of motion.

Table 15. Mean trial and mean phase indexes for the experimental subject group

Phase	Model	Mean Trial Index	Mean Phase Index
Starting	23	91.81	71.85
Constant	22	106.43	84.03
Stopping	21	110.52	76.73

In general, since model 2 under predicted the observed force for all subjects, the alpha adjustment improved the amplitude for all trials. Despite these trials being handicapped by not having the proper time lag adjustment, the mean trial and mean phase index values compare favorably with the previously found indexes . Tables 16 and 17 give the model with the lowest index value for each step of the analysis. Although these index values remain constant, indicating that no significant changes were made, the visual graphs show otherwise.

Table 16. Comparison of the lowest mean trial index values for the three steps of analysis

	Step 1		Step 2		Step 3	
Phase	Model	Index	Model	Index	Model	Index
Starting	2	102.19	23	90.33	23	91.81
Constant	2	105.22	22	114.21	22	106.43
Stopping	2	97.18	21	104.56	21	110.52

Table 17. Comparison of the lowest mean phase index values for the three steps of analysis

	Step 1		Step 2		Step 3	
Phase	Model	Index	Model	Index	Model	Index
Starting	2	83.38	24	67.25	23	71.85
Constant	3	84.25	21	85.94	22	84.03
Stopping	3	80.04	21	84.44	21	76.73

For trials in which the mean beta adjustment was close to the original, similar or better indexes were obtained. As shown in Figure 18, the improved amplitude prediction of model 23 also improves the index value (model 2 = 96.61, model 23 = 86.88) despite the time lag not being properly adjusted. Cases that tended to raise the index from the original value were the ones in which the initial beta adjustments were greater than one standard deviation away from the mean.

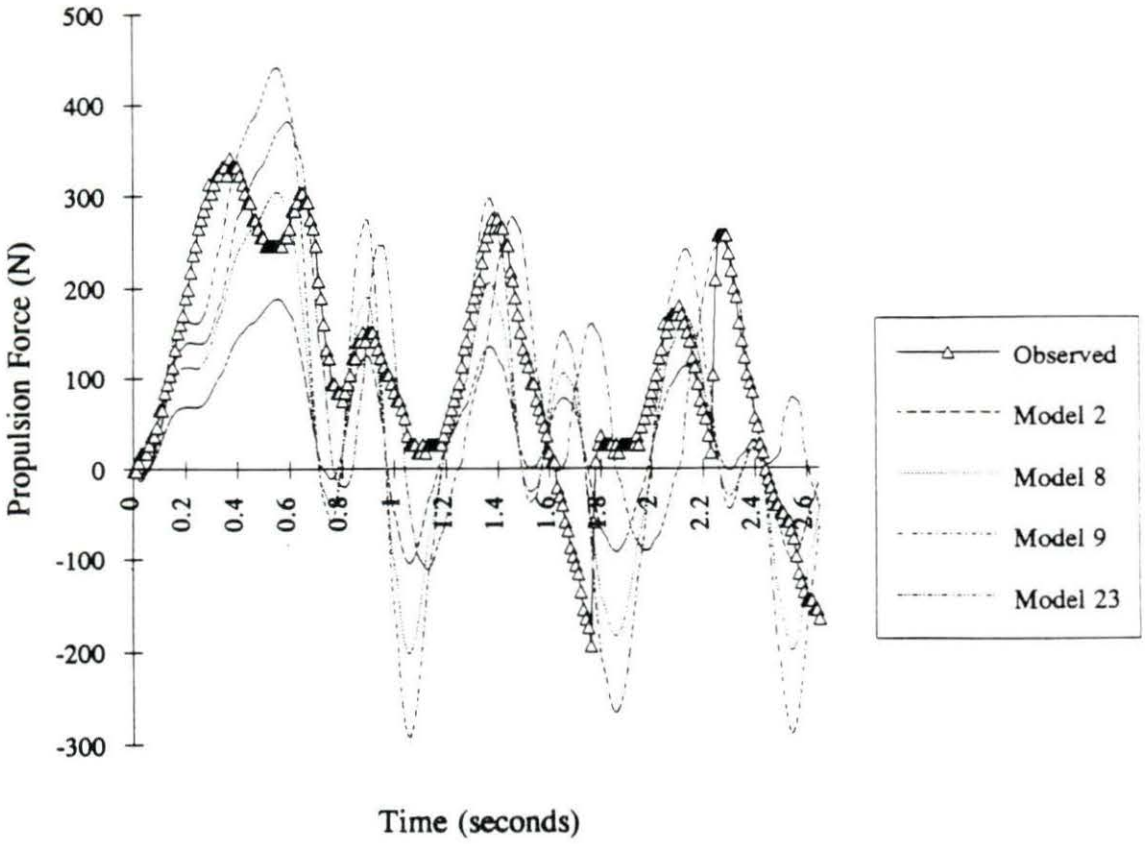

Figure 18. Improvement of amplitude prediction and index value despite improper time lag adjustment for subject GN trial 2 **Index values:** Model 2 - 96.61; model 8 - 94.96; model 9 - 111.15; model 23 - 86.88

CONCLUSION

The current investigation led to the conclusion that, in some form or another, the models found in literature are deficient in predicting standard wheelchair motion. The initial statistical analysis of these models showed that overall model 2, a derivation of Cooper's Model (1990c), was the best predictor of the observed forces. However, evidence from both visual comparisons and the model indexes of the individual trials showed otherwise. Some models predicted light subjects best (group A) whereas other predicted heavy subjects best (group C). A vertical adjustment factor, α, as a function a subject mass was generated to correct the deficiencies of the models.

The second set of models was established using model 2 as the equation of motion and adjusted by various degrees of alpha. It was found that the same model cannot be used to predict the each of the three phases of motion. The various magnitudes of alpha demonstrate the mechanical differences between the motion phases which must be considered. These mechanical differences were more important to the model than the air drag and bearing resistance terms which were found to be insignificant for slow wheelchair speeds.

Constant motion and stopping required the same alpha adjustment because subjects were in constant motion prior to stopping. The application of alpha to the deceleration values during the stopping phase helped predict the actual stop. Due to the mechanics involved in overcoming static friction and the large accelerations involved with starting, a larger alpha was needed for predicting observed starting forces. From these results it appears that a model's inability to predict peak to peak changes in force is a consequence of inconsistencies of propulsion of the subjects throughout a recorded trial. Averaging the profiles within a phase smoothed out some of the fluctuations as evident by the consistently lower mean phase indexes.

At this point, the validity of models 21, 22, and 23 lies within the weight range of the subjects tested. Since alpha was based on the subject weight range between 50 and 100 kilograms (110 to 220 pounds), it is unknown how subject masses outside of this range will affect propulsion and the outcome of the models. Recommendations for further studies include tests to verify these results with larger extremes of subject weight. In addition, by controlling the speed of the subjects, the relationship between how changes in acceleration, in terms of the different phases of motion, affect the model predicted force can be addressed. Finding this relationship may give insight for better prediction of peak to peak force changes and lead to a model that can better predict the inherent inconsistencies in real life standard wheelchair propulsion.

Because the alpha factor was required, it could be said that the original models fell short of their expectations of being valid predictors of wheelchair propulsion. However, it cannot be concluded that these models are invalid since they were generated for other purposes such as for racing wheelchairs or wheelchair ergometers. Wheelchair racers are well trained and display consistent strokes. On the other hand, wheelchair ergometers force a user to be consistent since a given work load or velocity must be maintained. Consequently, the original models may show excellent results, but they may not apply to every day situations.

Even though alpha was generated as a function of subject mass, the application of it as a correction factor was from a mathematical point of view with no physical meaning. The observed forces measured that had physical significance were the positive cycles that represented propulsion strokes. The negative deflections, considered as experimental error, cannot be modelled. Therefore, the application of alpha to positive values of acceleration (with the exception of model 21) rendered all models equal in terms of negative prediction. This approach yielded more credibility to

the index value as in indicator of the closeness of a model in terms of positive force prediction. The improvement of the alpha adjusted models over the first model set is demonstrated by comparable index values, better force amplitude prediction, and a more frequent occurrence of the model with the lowest index value also having the best amplitude prediction. Although further refinement of the second set models may lead to better results, it is believed that the models provided an accurate prediction of wheelchair propulsion based on the consistency of the mean trial and mean index values generated from each analysis step.

The validity of the equipment used is supported by the evidence given in the previous chapter. The linearity and high correlation coefficient of the calibration of the load cell give good indication of the consistency of the minigym in supplying resistance.

The load cell itself was set up to measure the force used to propel the wheelchair forward. Since the load cell was pre-loaded so that any additional force caused motion, it was expected that no negative forces would be obtained until the wheelchair stopped. The results obtained were not this ideal. Negative fluctuations between propulsion strokes are errors, whereas during stopping motion, the subject is ceasing wheelchair movement and the signal returns to the original zero line.

Measuring the acceleration and velocity via digitization techniques caused a problem in terms of the time differences. This problem could be avoided by including a large display digital clock in the camera field of view. Accurate measurement of time could then be accomplished by using the number of frames digitized and the actual time span to calculate the exact frequency of film rate for the digitization procedure. This process would have to be carried out for every trial. However, the key advantage to using the video process was that it required no physical attachments to the wheelchair and had no negative effects on wheelchair motion.

The analysis procedure was originally based on the calculation of a model index used as a mathematical estimation of the theoretical closeness each model prediction had with the observed force. After this initial analysis it was found that studying the index value alone was not sufficient. Visual comparisons of the force verses time was incorporated into the procedure to study the physical appearances of the profiles. The combination of the statistical and visual analysis led to the final models for estimating the starting , constant motion, and stopping phases of wheelchair propulsion.

Recommendations for further study include testing the model for predicting wheelchair motion on a slope and for various weight distributions. Since phase indexes show the same consistency as the trial indexes, single trials for subjects may be used, however better results will be obtained from averaging multiple trials. As mentioned above, further study should also include determining the relationship of acceleration with the models. A single model could be developed that would adapt to the stroke to stroke changes of real life propulsion. By using individuals with wheelchair experience, a higher level of propulsion consistency may be obtained.

BIBLIOGRAPHY

Beer, Ferdinand P. and Russell Johnston, Jr. 1984. Vector Mechanics for Engineers: Statics. 4th ed. McGraw-Hill Book Company, New York City, New York. 429 pages.

Brubaker, Clifford E. 1986. Wheelchair prescription: An analysis of factors that effect the mobility and performance. Journal of Rehabilitation Research and Development 23(4): 19-26.

Brubaker, Clifford E. 1988. Advances in wheelchair technology. IEEE Engineering in Medicine and Biology Magazine 7(3): 21-24.

Brubaker, Clifford E. 1990. Ergonometric considerations. Journal of Rehabilitation Research and Development, Clinical Supplement #2 27: 37-48.

Burkett, Lee N., J. Chisum, R. Cook, B. Norton, B. Taylor, K. Ruppert, and K. Wells. 1987. Construction and validation of a hysteresis brake wheelchair ergometer. Adapted Physical Activity Quarterly 4: 60-71.

Coe, Paul L, Jr. 1979. Aerodynamic characteristics of wheelchairs. NASA Technical Memorandum 80191. Langley Research Center, Hampton, Virginia.

Cooper, Rory A. 1989. Simulating wheelchair racing. Pages 450-451 in Proceedings of the 12th Annual RESNA Conference New Orleans, Louisiana.

Cooper, Rory A. 1990a. An exploratory study of racing wheelchair propulsion dynamics. Adapted Physical Activity Quarterly 7: 74-85.

Cooper, Rory A. 1990b. A force/energy optimization model for wheelchair athletics. IEEE Transactions on Systems, Man, and Cybernetics 20(2): 444-449.

Cooper, Rory A. 1990c. A systems approach to the modeling of racing wheelchair propulsion. Journal of Rehabilitation Research and Development 27(2): 151-162.

Cooper, Rory A. 1991. System identification of human performance models. IEEE Transactions on Systems, Man, and Cybernetics 21(1): 244-252.

Coutts, Kenneth D. 1990. Kinematics of sport wheelchair propulsion. Journal of Rehabilitation Research and Development 27(1): 21-26.

Coutts, Kenneth D., and Robert W. Schutz. 1988. Analysis of wheelchair track performances. Medicine and Science in Sports and Exercise. 20(2): 188-194.

Forcheimer, Fred, and Ake Lundberg. 1986. Wheelchair ergometer: Development of a prototype with electronic braking. Scandinavian Journal of Rehabilitation Medicine 18: 59-63.

Frank, T.G. and E.W. Abel. 1989. Measurement of the turning, rolling, and obstacle resistance of wheelchair castor wheels. Journal of Biomedical Engineering 11(6): 462-466.

Glaser, Roger, Steven R. Collins, and Stephan Wilde. 1980. Power output requirements for manual wheelchair locomotion. Proceedings of the National Aerospace Electronics Conference 2: 502-509.

Glaser, Roger M., and Steven R, Collins. 1981. Validity of power output estimation of wheelchair locomotion. American Journal of Physical Medicine 60(4): 180-189.

Gordon, John, James J. Kauzlarich, and John G. Thacker. 1989. Test of two new polyurethane foam wheelchair tires. Journal of Rehabilitation Research and Development 26(1): 33-46.

Harris, Tedric A. 1984. Rolling Bearing Analysis. 2nd ed. John Wiley and Sons, Inc., New York City, New York. 565 pages.

Higgs, Colin. 1983. An analysis of racing wheelchairs used at the 1980 Olympic Games for the disabled. Research Quarterly for Exercise and Sport 54(3): 229-233.

Higgs, Colin. 1984. Propulsion of racing wheelchairs. Pages 165-172 in Claudine Sherril eds. Sport and Disabled Athletes, Human Kinetics Publishers, Inc., Champaign, IL.

Jarvis, Stephen, and Hugh Rolfe. 1982. The use of an inertial dynamometer to explore the design of children's wheelchairs. Scandinavian Journal of Rehabilitation Medicine 14: 167-176.

Johnson, Barry W. , and James H. Aylor. 1985. Dynamic modeling of an electric wheelchair. IEEE Transaction on Industry Applications IA 21(5): 1284-1293.

Krepchin, Ira P. 1982. How to calculate rolling resistance. Modern Materials Handling 41(5): 72.

Lakomy, H.K.A., I. Campbell, and C. Williams. 1987. Treadmill performance and selected physiological characteristics of wheelchair athletes. British Journal of Sports Medicine 21(3): 130-133.

Lemaire, Edward D., M. Lamontagne, H. Barclay, T. John, and G. Martel. 1991. A technique for the determination of center of gravity and rolling resistance for tilt seat wheelchairs. Journal of Rehabilitation Research and Development 28(3): 51-58.

Masse, L.C. and M. Lamontagne. 1990. Kinematic analysis of wheelchair propulsion for three speeds of propulsion. Abstract #234 in Robert J. Gregor, and et. al. XII International Congress of Biomechanics: Congress Proceedings, UCLA, Los Angeles, CA.

McLaurin, C.A., and C.E. Brubaker. 1991. Biomechanics and the wheelchair. Prosthetics and Orthotics International 15: 24-37.

Mattison, Paul G., John Hunter, and Sheena Spence. 1989. Development of a realistic method to assess wheelchair propulsion by disabled people. International Journal of Rehabilitation Research 12(2): 137-145.

Niesing, R., F. Eijskoot, R.Kranse, A.H. den Ouden, J.Storm, H.E.J. Veeger, L.H.V. Van der Woude, and C.J Snijders. 1990. Computer-controlled wheelchair ergometer. Medical and Biological Engineering and Computing 28: 329-338.

Phillips, G.J. 1988. Using the ball bearing as a force transducer. Experimental Techniques 12(12): 32-34

Ridgeway, Mary, Carol Pope, and Jerry Wilkerson. 1988. A kinematic analysis of 800-meter wheelchair racing techniques. Adapted Physical Activities Quarterly 5: 96-107.

Samuelsson, Kersti, H. Larson, and Hans Tropp. 1991. Power output and propulsion technique in wheelchair driving. International Journal of Rehabilitation Research 14(1): 76-81.

Sanderson, David J. and H.J.Sommer III. 1985. Kinematic features of wheelchair propulsion. Journal of Biomechanics 18(6): 423-429.

Thacker, J.G., J.R. O'Reagan, J.H. Aylor. 1980. A wheelchair dynamometer. Transactions of the ASME - Journal of Mechanical Design 102: 718-722.

Van der Woude, L.H.V., G. deGroot, A.P. Hollander, G.J. Van Ingen Schenau and R.H. Rozendal. 1986. Wheelchair ergonomics and physiological testing of prototypes. Ergonomics 29(6): 1561-1573.

Van der Woude, L.H.V., K.M. Hendrich, H.E.J. Veeger, G.J. van Ingen Schenau R.H. Rozendal, G. deGroot, and A.P. Hollander. 1988a. Manual wheelchair propulsion: Effects of power output on physiology and technique. Medicine and Science in Sports and Exercise 20(1): 70-78.

Van der Woude, L.H.V., H.E.J. Veeger, R.H. Rozendal, G.J. van Ingen Schenau, F. Rooth, and P. van Nierop. 1988b. Wheelchair racing: Effects of rim diameter and speed on physiology and technique. Medicine and Science in Sports and Exercise 20(5): 492-500.

Van der Woude, L.H.V., Dirk-Jan Veeger, R.H. Rozendal, and T.J. Sargeant. 1989. Seat height in handrim wheelchair propulsion. Journal of Rehabilitation Research and Development 26(4): 31-50.

Van Ingen Schenau, G.J. 1980. Some fundamental aspects of the biomechanics of overground versus treadmill locomotion. Medicine and Science in Sports and Exercise 12(4): 257-261.

Veeger, H.E.J., L.H.V. van der Woude, and R.H. Rozendal 1989. The effect of rear wheel camber in manual wheelchair propulsion. Journal of Rehabilitation Research and Development 26(2): 37-46.

Walsh, C.M., G.E. Marchiori, and R.D. Steadward. 1986. Effect of seat position on maximal linear velocity in wheelchair sprinting. Canadian Journal of Applied Sport Sciences 11(4): 186-190.

Wood, Graeme A. 1982 Data smoothing and differentiation procedures in biomechanics. in Ronald L Terjung Exercise and Sport Sciences Review vol. 10 of American College of Sports Medicine Series. Pages 308-362.

ACKNOWLEDGEMENTS

I would like to thank my major professor, Dr. Patrick Patterson, for his advice and guidance during this research, and Doctors H.T. David and David Carlson for serving on my committee. I want to express my appreciation to these professors for their consideration, pleasant disposition, and constant willingness to help.

I would also like to thank the following people for their help during the course of this project: 1) Doctors L. Zachary and K. McConnell in Engineering Mechanics for their technical expertise and the use of the load cell, oscilloscope, and accessories, 2) Dr. D. Cox in Statistics who assisted with data analysis, and 3) Mary Greely Rehabilitation Center for the use of their Minigym.

Finally, and most importantly, I want to express my deepest gratitude to my parents, Richard and Mary Hofstad, and to my grandfather, Myron Lee, for their continual support and guidance.

APPENDIX A: FORTRAN PROGRAMS AND MODEL VARIATIONS

FORTRAN Programs

Program 1: Observed force and calibration data preparation program

```
      PROGRAM BASELINE
C
C  THIS PROGRAM READS THE FIRST TEN LINE OF THE INPUT FILE
C  (TRIAL.DAT) AND WRITES THEM TO A BASELINE FILE (BASE.DAT). THE
C  INPUT FILE IS REWOUND AND SYSTEMATICALLY SUBTRACTED FROM
C  THE BASELINE FILE. THE OUTPUT FILE IS DIFFEREN.DAT
      DIMENSION DATA(199,20)
      DIMENSION BASE(10,20)
      INTEGER DATA,BASE,B,D1,D2,D3,D4,D5,D6,D7,D8,D9
      INTEGER D10,D11,D12,D13,D14,D15,D16,D17,D18,D19,D20
      OPEN(UNIT=10,FILE='TRIAL.DAT',STATUS='OLD')
      OPEN(UNIT=11,FILE='BASE.DAT',STATUS='UNKNOWN')
      OPEN(UNIT=21,FILE='DIFFEREN.DAT',STATUS='UNKNOWN')
      B=0
C
C  READ FIRST TEN LINES OF INPUT FILE AND WRITE TO BASE.DAT
C
      DO 100 I = 1,10
           READ(10,*)(BASE(I,J), J=1,20)
           WRITE(11,3)BASE(I,1),BASE(I,2),BASE(I,3),BASE(I,4),BASE(I,5),
     #          BASE(I,6),BASE(I,7),BASE(I,8),BASE(I,9),BASE(I,10),
     #          BASE(I,11),BASE(I,12),BASE(I,13),BASE(I,14),BASE(I,15),
     #          BASE(I,16),BASE(I,17),BASE(I,18),BASE(I,19),BASE(I,20)
 3         FORMAT(1X,I3,1X,I3,1X,I3,1X,I3,1X,I3,1X,I3,1X,I3,1X,I3,1X,I3,1X,I3,1X,I3,
     #          1X,I3,1X,I3,1X,I3,1X,I3,1X,I3,1X,I3,1X,I3,1X,I3,1X,I3,1X,I3,1X,I3)
 100  CONTINUE
      REWIND(UNIT=10)
 5    REWIND(UNIT=11)
C
C  READ INPUT FILE AND SUBTRACT FROM BASELINE (BASE.DAT)
C
      DO 200 I = 1,10
        READ(10,*)(DATA(I,J), J=1,20)
             D1=DATA(I,1) - BASE(I,1)
             D2=DATA(I,2) - BASE(I,2)
```

```
                D3=DATA(I,3) - BASE(I,3)
                D4=DATA(I,4) - BASE(I,4)
                D5=DATA(I,5) - BASE(I,5)
                D6=DATA(I,6) - BASE(I,6)
                D7=DATA(I,7) - BASE(I,7)
                D8=DATA(I,8) - BASE(I,8)
                D9=DATA(I,9) - BASE(I,9)
                D10=DATA(I,10) - BASE(I,10)
                D11=DATA(I,11) - BASE(I,11)
                D12=DATA(I,12) - BASE(I,12)
                D13=DATA(I,13) - BASE(I,13)
                D14=DATA(I,14) - BASE(I,14)
                D15=DATA(I,15) - BASE(I,15)
                D16=DATA(I,16) - BASE(I,16)
                D17=DATA(I,17) - BASE(I,17)
                D18=DATA(I,18) - BASE(I,18)
                D19=DATA(I,19) - BASE(I,19)
                D20=DATA(I,20) - BASE(I,20)
            OPEN(UNIT=11, FILE='BASE.DAT',STATUS='OLD')
            READ(11,*)(BASE(I,J), J=1,20)
C
C  WRITE NEW DATA TO AN OUTPUT FILE (DIFFEREN.DAT)
C
            WRITE(21,7)D1,D2,D3,D4,D5,D6,D7,D8,D9,D10,D11,D12,D13,
     #          D14,D15,D16,D17,D18,D19,D20
  7         FORMAT(1X,I3,1X,I3,1X,I3,1X,I3,1X,I3,1X,I3,1X,I3,1X,I3,1X,I3,1X,I3,1X,I3,
     #          1X,I3,1X,I3,1X,I3,1X,I3,1X,I3,1X,I3,1X,I3,1X,I3,1X,I3,1X,I3,1X,I3)
  200 CONTINUE
C
C  REPEATS PROCESS FOR NEXT SET OF TEN LINES OF INPUT FILE AND
C  CONTINUES UNTIL ALL 200 LINES OF THE INPUT FILE HAVE
C  BEEN PROCESSED.
C
      B=B+1
      IF(B.LT.20)THEN
         GO TO 5
         ENDIF
      END
```

Program 2: Observed force conversion program

```
      PROGRAM WEIGHT
C
C THIS PROGRAM CONVERTS THE GRABBER POINT NUMBER TO THE
C EQUIVALENT WEIGHT VALUE AND SUBTRACTS OUT THE MINIGYM
C FACTOR (5.76 LBS). RESULTING VALUE ARE IN NEWTONS.
C
      DIMENSION GRAB(200,20)
      DIMENSION DATA(200,20)
      REAL*8 DATA
      INTEGER GRAB,I,J
C
      OPEN(UNIT=20,FILE='LOAD.DAT',STATUS='OLD')
      OPEN(UNIT=21,FILE='NEWT.DAT',STATUS='NEW')
C
      READ(20,*)((GRAB(I,J),J=1,20),I=1,199)
        DO 200 I=1,199
           DO 100 J=1,20
              DATA(I,J)=((GRAB(I,J)*2.1464 + 3.2206)-5.76)*4.448
              WRITE(21,50)DATA(I,J)
50            FORMAT(1P,E10.3)
100        CONTINUE
200     CONTINUE
        END
```

Program 3: Force prediction program

```
      PROGRAM MODEL
C
C THIS PROGRAM OPENS A DATA FILE UNDER THE NAME 'ACC.DAT'
C AND ASKS FOR THE OTHER INPUT VARIABLES TO BE USED IN THE
C WHEELCHAIR MODEL. IT CALCULATES THE FORCE REQUIRED TO
C PROPEL A WHEELCHAIR OVER FLAT GROUND. THE FORCE OUTPUT
C AND ALL OF THE INPUT VALUES ARE THEN STORED IN A 'FORCE.DAT'
C FILE FOR ANALYSIS PURPOSES.
C
      DIMENSION DATA(300,4)
      REAL*8 RR,RPR,IR,IFW,RF,C,K,BRR,BRF,W,MR,MF,WR,WF,Z,
```

```
      REAL*8 DATA,PERCENT
      CHARACTER PHASE*4,PATH*8,DATE*20
C
C THE FOLLOWING OPENS THE INPUT DATA FILE, CREATES THE
C OUTPUT FORCE FILE AND ASKS FOR RELATIVE BACKGROUND
C INFORMATION.
C
      OPEN(UNIT=14,FILE='ACC.DAT',STATUS='OLD')
      REWIND(UNIT=14)
      OPEN(UNIT=15,FILE='FORCE.DAT',STATUS='UNKNOWN')
C
      WRITE(*,10)
 10   FORMAT(1X,' What is the name of the file? ')
      READ(*,'(A)') FORM
      WRITE(15,20)FORM
 20   FORMAT(1X,'Filename: ',A20,/)
C
      PRINT*,' What is today's date? '
      READ(*,'(A)')DATE
      WRITE(15,30)DATE
 30   FORMAT(1X,'Date: ',A20,/)
C
C SPECIFY THE PHASE OF MOTION
C
      PRINT*,' What is the phase of motion?'
      PRINT*,' If starting phase, type A.'
      PRINT*,' If constant motion, type B.'
      PRINT*,' If stopping, type C.          '
      READ(*,'(A)')PHASE
      IF((PHASE.EQ.'A').OR.(PHASE.EQ.'a'))THEN
            WRITE(15,40)
 40         FORMAT(1X,'Phase: STARTING',/)
      ELSEIF((PHASE.EQ.'B').OR.(PHASE.EQ.'b'))THEN
            WRITE(15,50)
 50         FORMAT(1X,'Phase: CONSTANT MOTION',/)
      ELSE
            WRITE(15,60)
 60         FORMAT(1X,'Phase: STOPPING',/)
```

```
      ENDIF
C
C  INPUT VARIABLES:
C  RR = RADIUS OF REAR WHEELS
C  RPR = RADIUS OF PUSH RINGS
C  IR = INERTIA OF REAR WHEELS
C  IFW = INERTIA OF FRONT WHEELS
C  RF = RADIUS OF FRONT WHEELS
C  C = DRAG COEFFICIENT
C  KV = BEARING RESISTANCE
C  BRR = COEFFICIENT OF REAR ROLLING RESISTANCE
C  BRF = COEFFICIENT OF FRONT ROLLING RESISTANCE
C  W = WEIGHT OF INDIVIDUAL AND WHEELCHAIR
C  WR = WEIGHT ON REAR WHEELS
C  WF = WEIGHT ON FRONT WHEELS
C  MR = MASS OF ONE REAR WHEEL
C  MF = MASS OF ONE FRONT WHEEL
C  Z = PREDICTED FORCE
C
C  SPECIFY THE INPUT FOR THE SUBJECT VARIABLES
C

      PRINT*,' Do you want to input new subject variables? (y or n) '
      READ(*,'(A)')PATH
      IF((PATH.EQ.'n').OR.(PATH.EQ.'N'))THEN
            OPEN(UNIT=16,FILE='USER.DAT',STATUS='UNKNOWN')
            REWIND(UNIT=16)
            READ(16,*)W,WR,WF,PERCENT
            GO TO 130
      ELSE
            OPEN(UNIT=16,FILE='USER.DAT',STATUS='UNKNOWN')
            PRINT*,' Enter the following variables.'
      ENDIF
C
      WRITE(*,70)
 70   FORMAT(1X,' What is the weight of the user and the wheelchair? ')
      READ(*,80)W
 80   FORMAT(BN,F10.3)
```

```
      PRINT*,' What percent of the weight is on the rear wheels? '
      READ(*,95)PERCENT
 95   FORMAT(-2P,F5.2)
      WR = (PERCENT*W)/100
      WRITE(*,100)WR
C
C CALCULATES THE WEIGHT DISTRIBUTION ON FRONT AND REAR
C WHEELS GIVEN THE PERCENT SPECIFIED.
C
 100  FORMAT(5X,' The weight on the rear wheels is: ',F10.3,' N',/)
      WF = W-WR
      WRITE(*,110)WF
 110  FORMAT(5X,' The weight on the front wheels is: ',F10.3,' N',/)
      WRITE(16,120)W,WR,WF,PERCENT
 120  FORMAT(1X,E10.3,2X,E10.3,2X,E10.3,2X,F5.2)
C
C SPECIFY THE WHEELCHAIR VARIABLES
C
 130  PRINT*,' Do you want to input new wheelchair variables? (y or n) '
      READ(*,'(A)')PATH
      IF((PATH.EQ.'n').OR.(PATH.EQ.'N'))THEN
              OPEN(UNIT=17,FILE='CHAIR.DAT',STATUS='UNKNOWN')
              REWIND(UNIT=17)
              READ(17,*)RR,RF,RPR,IR,IFW
        GO TO 250
      ELSE
              OPEN(UNIT=17,FILE='CHAIR.DAT',STATUS='UNKNOWN')
              PRINT*,' Enter the following variables.'
      ENDIF
C
      WRITE(*,140)
 140  FORMAT(1X,'What is the rear wheel radius? ')
      READ(*,150)RR
 150  FORMAT(BN,E10.3)
      WRITE(*,160)
 160  FORMAT(1X,'What is the front wheel radius? ')
      READ(*,170)RF
 170  FORMAT(BN,E10.3)
```

```
      WRITE(*,180)
  180 FORMAT(1X,'What is the push ring radius? ')
      READ(*,190)RPR
  190 FORMAT(BN,E10.3)
      WRITE(*,200)
  200 FORMAT(1X,'What is the mass of one rear wheel? ')
      READ(*,210)MR
  210 FORMAT(BN,F10.3)
      IR = 2*MR*(RR**2)
      WRITE(*,220)
  220 FORMAT(1X,'What is the mass of one front wheel? ')
      READ(*,230)MF
  230 FORMAT(BN,F10.3)
      IFW = 2*MF*(RF**2)
      WRITE(17,240)RR,RF,RPR,IR,IFW
  240 FORMAT(1X,5E10.3)
C
C SPECIFY THE COEFFICIENTS AND RESISTANCES
C
  250 PRINT*,'Do you want to input new resistances? (y or n) '
      READ(*,'(A)')PATH
      IF((PATH.EQ.'n').OR.(PATH.EQ.'N'))THEN
      OPEN(UNIT=18,FILE='COEF.DAT',STATUS='UNKNOWN')
            REWIND(UNIT=18)
            READ(18,*)C,K,BRR,BRF
            GO TO 345
      ELSE
            OPEN(UNIT=18,FILE='COEF.DAT',STATUS='UNKNOWN')
            PRINT*,' Enter the following variables.'
      ENDIF
C
      WRITE(*,260)
  260 FORMAT(1X,'What is the drag coefficient? ')
      READ(*,270)C
  270 FORMAT(BN,F10.3)
      WRITE(*,280)
  280 FORMAT(1X,'What it the bearing resistance? ')
      READ(*,290)K
```

```
290 FORMAT(BN,F10.3)
    WRITE(*,300)
300 FORMAT(1X,'What is the rear rolling resistance coefficient? ')
    READ(*,310)BRR
310 FORMAT(BN,F10.3)
    WRITE(*,320)
320 FORMAT(1X,'What is the front rolling resistance coefficient? ')
    READ(*,330)BRF
330 FORMAT(BN,F10.3)
    WRITE(18,340)C,K,BRR,BRF
340 FORMAT(1X,4E10.3)
C
C ALL INPUT VARIABLES ARE WRITTEN TO AN OUTPUT FILE AS WELL
C AS THE INPUT DATA FILE AND THE FORCE PREDICTIONS.
C
345 WRITE(15,360)
360 FORMAT(26X,'INPUT PARAMETERS')
    WRITE(15,370)
370 FORMAT(25X,'----------',/)
    WRITE(15,380)W
380 FORMAT(1X,'Total weight of the user and wheelchair: ',F8.3,' Kilograms')
    WRITE(15,390)WR,WF
390 FORMAT(5X,'Rear wheel weight: ',F8.3,' Kilograms',5X,/
   #        5X,'Front wheel weight: ',F8.3,' Kilograms')
    WRITE(15,395)PERCENT,100.0-PERCENT
395 FORMAT(5X,'The ratio of the rear to front weight is: ',
   #        F5.2,'/',F5.2,/)
    WRITE(15,400)
400 FORMAT(1X,'Radii of the wheelchair wheels:')
    WRITE(15,410)RR,RF,RPR
410 FORMAT(5X,'Rear wheel: ',F8.3,' Meters',/
   #        5X,'Front wheel: ',F8.3,' Meters',/
   #        5X,'Push-ring: ',F8.3,' Meters',/)
    WRITE(15,420)
420 FORMAT(1X,'Inertia of the wheels: (calculated from I=mR^2)')
    WRITE(15,430)IR,IFW
430 FORMAT(5X,'Rear wheels combined: ',F7.4,' Kg*m^2',/
   #        5X,'Front casters combined: ',F7.4,' Kg*m^2',/)
```

```
      WRITE(15,440)
 440  FORMAT(1X,'Coefficients and Resistances:')
      WRITE(15,450)C,K,BRR,BRF
 450  FORMAT(5X,'Drag coefficients: ',F7.4,/
     #        5X,'Bearing resistance: ',F7.4,/
     #        5X,'Coefficient of rear rolling resistance: ',F7.4,/
     #        5X,'Coefficient of front rolling resistance: ',F7.4,/)
C
C  FORMAT THE HEADINGS FOR THE OUTPUT SCREEN DISPLAY.
C
      WRITE (*,530)
 530  FORMAT(3X,'TIME',10X,'DISTANCE',6X,'VELOCITY',5X,
     #        'ACCELERATION',4X,'FORCE')
      WRITE (*,540)
 540  FORMAT(3X,'(sec)',11X,'(m)',10X,'(m/s)',8X,'(m/sec^2)',7X,'(N)')
C
C  FORMAT THE HEADINGS FOR THE OUTPUT FILE.
C
      WRITE(15,550)
 550  FORMAT(4X,'TIME',8X,'DISTANCE',6X,'VELOCITY',4X,
     #        'ACCELERATION',5X,'FORCE')
      WRITE(15,560)
 560  FORMAT(4X,'(sec)',10X,'(m)',10X,'(m/s)',7X,'(m/sec^2)',7X,'(N)')
C
C  READS THE DATA FROM THE INPUT FILE IN ORDER (TIME, DISTANCE
C  VELOCITY, AND ACCELERATION). ONE LINE AT A TIME AND
C  CALCULATES THE FORCE.  NOTE:  DATA FROM INPUT FILE HAS UNITS
OF CENTIMETERS AND IS CONVERTED TO METERS IN THE EQUATION
C
      OPEN(UNIT=20,FILE='FINAL.DAT',STATUS='NEW')
      DO 600 I = 1,300
         READ(14,*)(DATA(I,J), J=1,4)
 570     FORMAT(BN,4E10.4)
         Z=(RPR/RR)*((W+IR/(RR**2)+IFW/(RF**2))*(DATA(I,4)*0.01)
     #        +C*((DATA(I,3)*0.01)**2) + K*(DATA(I,3)*0.01)
     #        +((WR*BRR/RR)+(WF*BRF/RF))*(DATA(I,2)*0.01))
         WRITE(*,580)DATA(I,1),DATA(I,2)*0.01,DATA(I,3)*0.01,
     #        DATA(I,4)*0.01,Z
```

```
580     FORMAT(1P,E10.3,4X,E10.3,4X,E10.3,4X,E10.3,4X,E10.3)
        WRITE(15,590)DATA(I,1),DATA(I,2)*0.01,DATA(I,3)*0.01,
  #        DATA(I,4)*0.01,Z
590     FORMAT(1P,E10.3,4X,E10.3,4X,E10.3,4X,E10.3,3X,E12.5)
        WRITE(20,595)Z
595     FORMAT(1P,E10.3)
600  CONTINUE
610  ENDFILE(UNIT=14)
615  ENDFILE(UNIT=15)
620  ENDFILE(UNIT=16)
625  ENDFILE(UNIT=17)
630  ENDFILE(UNIT=18)
640  ENDFILE(UNIT=20)
       END
```

Variations on the Model

Model 1°[1]

$$Z = (RPR/RR)*[(W + IR/RR^2 + IFW/RF^2)*A + C*V^2 + K*V + (WR*BRR/RR + WF*BRF/RF)*X)]$$

Model 2°

$$Z = (RPR/RR)*[(W + IR/RR^2 + IFW/RF^2)*A + (0.5*D*O*C*(VW-V^2)) + (WR*BRR/RR + WF*BRF/RF)*X]$$

Model 3°

$$Z = (RPR/RR)*[(W + IR/RR^2 + IFW/IF^2)*A + K*V + (0.5*D*O*C*(VW-V^2)) + (WR*BRR/RR + WF*BRF/RF)*X]$$

Model 4°

$$Z = (RPR/RR) * [(W + IR/RR^2 + IFW/RF^2)*A + C*(V^2) + (WR*BRR/RR + WF*BRF/RF)*X]$$

° Denotes models used for analysis.

[1] Model involved with program 3 on page ?

Model 5

$$Z = (RPR/RR) * [(W + IR/RR^2 + IFW/RF^2)*A + C*V^2 + K*V + (2*FUR + 2*FUF)*9.8*A]$$

Model 6

$$Z = (RPR/RR) * [(W + IR/RR^2 + IFW/RF^2)*A + C*V^2 + K*V + (2*FUR + 2*FUF)*A]$$

Model 7

$$Z = (RPR/RR)*[(W + IR/RR^2 + IFW/RF^2)*A + C*V^2 + K*V + (FUR+FUF)*A]$$

Model 8°

$$Z = (RPR/RR) * [W*A + C*V^2 + K*V + (FUR + FUF)*A]$$

Model 9°

$$Z = (RPR/RR) * [W*A + C*V^2 + K*V + (2*FUR + 2*FUF)*A]$$

Model 10°

$$Z = (RPR/RR) * [W*A + (FUR + FUF)*A]$$

Model 11

$$Z = (RPR/RR) * [W*A + C*V^2 + (FUR + FUF)*A]$$

Model 12

$$Z = (RPR/RR) * [W*A + K*V + (FUR + FUF)*A]$$

Model 13°

$$Z = (RPR/RR) * [(W + IR/RR^2 + IFW/RF^2)*A + (WR*BRR/RR + WF*BRF/RF)*X]$$

Model 14

$$Z = (RPR/RR) * [(W + IR/RR^2 + IFW/RF^2)*A + C*V^2 + K*V + (2*FUR + 2*FUF)*9.8*A]$$

Nomenclature for All the Models Used

A = Acceleration of the wheelchair.
BRF = Coefficient of front rolling resistance.
BRR = Coefficient of rear rolling resistance.
C = Coefficient of air drag.
D = Density of air.
FUF = Front wheel friction
FUR = Rear wheel friction
IFW = Inertia of the front wheels.
IR = Inertia of the rear wheels.
KV = Coefficient of bearing resistance.
LWB = Wheelbase length
MF = Weight of one front wheel.
MR =weight of one rear wheel.
O = Frontal area of the user/wheelchair system.
RCG = Distance from center of gravity to rear wheel axle.
RF = Radius of the front wheels.
RPR = Radius of the push rings.
RR = Radius of the rear wheels.
V = velocity of the wheelchair.
VW = velocity of the wind.
W = Weight of the individual and the wheelchair.
WF = Weight on the front wheels.
WR = Weight on the rear wheels.
X = Distance traveled.
Z = Model predicted force.

Additional equations used in models but not found in program model

$RCG = (W - 17.73)*0.171$

$FUR = BRR * (W - (RCG*W)/LWB)$

$FUF = BRF * ((RCG*W)/LWB)$

where:

17.73 = Weight of wheelchair in kilograms
0.171 = Correction factor for subject weight differences.

Sample of Subject Data for Possible Clinical Evaluation

Filename: Subject Name

Date: 12/04/92

Phase: STARTING

INPUT PARAMETERS

Total mass of the user and wheelchair: 111.00 Kilograms
Rear wheel weight: 66.60Kilograms
Front wheel weight: 44.40Kilograms
The ratio of the rear to front weight is: 60.00/40.00

Radii of the wheelchair wheels:
Rear wheel: 0.305 Meters
Front wheel: 0.102 Meters
Push-ring: 0.273 Meters

Inertia of the wheels: (calculated from I=mR^2)
Rear wheels combined: 0.426 Kg*m^2
Front casters combined: 0.00749 Kg*m^2

Coefficients and Resistances:
Drag coefficients: 1.4000
Coefficient of bearing resistance: 0.06
Coefficient of rear rolling resistance: 0.0110
Coefficient of front rolling resistance: 0.0410

Time (sec)	Distance (m)	Velocity (m/sec)	Acceleration (m/sec^2)	Force (N)
0.000E+00	1.000E-03	-3.000E-03	3.100E-02	3.24514E+00
1.000E-02	1.000E-03	-3.000E-03	7.400E-02	7.68509E+00
2.000E-02	1.000E-03	-1.000E-03	2.080E-01	2.16341E+01
3.000E-02	1.000E-03	3.000E-03	3.700E-01	3.84979E+01
4.000E-02	1.000E-03	9.000E-03	5.510E-01	5.73396E+01
5.000E-02	1.000E-03	1.600E-02	7.440E-01	7.74304E+01

APPENDIX B: PROPOSAL AND CONSENT FORM FOR USE OF HUMAN SUBJECTS

Proposal

Validation and extension of a biomechanical model of wheelchair propulsion

A. Problem to be examined

The intent of this project is to study the dynamics of wheelchair propulsion, specifically the force applied to the push rims of a wheelchair and the resulting acceleration, velocity and distance traveled. This information will be used to validate an existing computer model of wheelchair propulsion. Measurements for this project will be taken simultaneously by two sets of equipment: a load cell system and a video camera system.

The force applied will be measured by a load cell attached to the frame of the wheelchair on the underside of the seat. The transducer will be supported by a sling hanging from the back rest. The other end of the load cell will be attached to a Minigym, an isokinetic exercise device offering constant resistance to pull. The load cell measures the tension in the rope between the Minigym and the wheelchair as it is propelled across the floor. The Minigym will be locked into place by a floor tie-in mechanism. Two pieces of instrumentation will be used to collect the data from the load cell: (1), an oscilloscope will sample the data and show an immediate display of what is happening, and (2), a computer to capture the values from the oscilloscope and store them in a file.

The motion of the subjects as they propel the wheelchair across the floor will be video taped to obtain the acceleration, velocity, and distance profiles through digitization techniques. Nine passes in front of the camera for each subject will be used: three passes for each phase of motion. Computer digitization of the video tape will provide the said profiles as well as the motion of the head, shoulders, arms, and trunk involved to facilitate conclusions drawn on the dynamic results. Between each trial the wheelchair will be returned to the starting point making sure that the Minigym line recoils properly and the load cell cable is not strained.

B. Characteristics of the subjects.

Number: 8.
Age Range: 18 to 55.
Sex: Male and Female.
Location: From Ames Area.

It is desired to have experienced wheelchair users take part in the experiment, although able-bodied subjects may need to be used as well to get the desired numbers. No incentives will be offered; this is a one time experiment for each subject. If the subjects desire, I will provide them with their own results upon completion of the analysis.

C. Risks and Discomforts.

Transfers: In the case that a handicapped subject must use the provided wheelchair, they must transfer into it. Help for a transfer will be offered and carried out under the instruction of the subject. Alternatives to using the provided chair include connecting the load cell to the subjects wheelchair with their permission. If it is impossible to connect the load cell, or the subject does not want it connected, the subject can decline participation. Connecting the load cell to the wheelchair can be done with the subject seated.

Physical strain: Physical exercise is involved and is explained below. If the subject cannot propel against the resistance, either the resistance will be lowered or they can choose to discontinue the experiment.

Reversing: To get from the end of one trial to the beginning of the next, the subject must propel backwards to the starting point. Directions and instructions for this process will be explained and assistance will be offered. An alternative to reversing is to disconnect the load cell thus allowing the subject to freely propel the wheelchair back to the starting point.

This experiment will take place in the Veterinary Medicine Building, which is accessible to the handicapped. In the cases where able-bodied subjects are used, transfers will not be a risk. Prior to getting into the wheelchair, instructions on its use will be provided. For all subjects, these instructions will also include what is being observed during the test. Additional instructions on the use of the wheelchair will be provided for the able-bodied subjects.

D. Additional Information

A minimal amount of physical exercise is involved. The extent will be traveling across the floor a distance of 25 feet in a wheelchair for the three trials plus any practice runs the subject needs. The wheelchair will be connected to a constant resistance set at a minimal value so the propulsion force will be slightly higher than normal. The desired speed attained for the tests will be an average, everyday cruising speed.

Consent Form

Signed informed consent for validation and extension of a biomechanical model of wheelchair propulsion

1. The intent of this project is to study the dynamics of wheelchair propulsion. We want to know the force applied to the push rims of a wheelchair and the resulting acceleration, velocity and distance traveled. The test involves the propulsion of a wheelchair across the floor in order to study the three phases of motion: starting, constant velocity, and stopping. The wheelchair will be connected to a constant resistance source so a load cell can measure the tension in the rope. At the same time, a video camera will be taping the motion. From the tape, the acceleration, velocity and distance of the process will be determined along with an analysis of the upper body movement. All of this information will be used to validate a computer model of wheelchair propulsion.

The role of the subject is to propel the wheelchair in a straight line a distance of 25 feet across the floor. You may take some practice trials prior to the testing to get a feel for the added tension. Nine test trials in which data is recorded is preferred.

2. Physical exertion against a constant resistance is required. This resistance is kept to a minimum and can be lowered if desired.

3. There are no incentives to do this experiment.

4. Alternative procedure to the test is to lower the resistance in the Minigym. If it is too strenuous to propel the wheelchair or you think three times will be too much effort, resistance can be lowered or the tests can be terminated.

5. Feel free to ask any question concerning the procedure or the experiment in general.

6. You agreement to participate is not a binding contract that says you must complete the task. You are free to withdraw your consent, and discontinue participation at any time.

7. All information will be kept confidential. You name will not appear in any publication or thesis but the results of the force, acceleration, velocity, and distance will. The video tapes made of the subject will be shown to researchers only, and will be erased at the conclusion of the study.

8. The amount of time required of each subject is 45 - 60 minutes.

9. Emergency treatment of any injuries that may occur as a direct result of participation in this research will be treated at the Iowa State University student Health Services, Student Services Building, and/or referred to Mary Greeley Hospital or another physician. Compensation for treatment of any injuries that may occur as a direct result of participation in this research may or may not be paid by Iowa State University depending on the Iowa Tort Claims Act. Claims for compensation will be handled by the Iowa State University Vice President for Business and Finance.

By signing below you state that you have read this consent form, understand it, have had your questions pertaining to it satisfactorily answered, and voluntarily agree to participate in this study accepting the risks entailed by it. You also understand that you may discontinue participation at any time for any reason without objection by the researchers or anyone involved with the study.

Volunteer Subject: _____

Researcher/ Witness: _____

APPENDIX C: STATISTICAL MODEL INDEX VALUES GENERATED FOR EACH SET OF MODELS

Table 18. Model set 1 trial 1 index values (starting phase)

Subject	Model 1	Model 2	Model 3	Model 4	Model 8	Model 9	Model 10	Model 13
KH	No Data							
GN	138.92	136.98	137.91	138.93	131.20	135.89	131.90	139.64
VD	125.56	124.94	125.86	125.58	121.03	116.66	121.64	126.17
SK	103.25	102.03	102.67	103.26	95.74	83.14	96.37	103.80
BF	96.53	94.58	94.84	96.57	151.21	278.25	150.37	96.80
CO	76.53	77.31	77.49	76.53	157.22	300.28	157.00	70.85
RK	110.19	110.91	110.90	111.40	118.86	212.61	118.69	110.41

Table 19. Model set 1 trial 2 index values (starting phase)

Subject	Model1	Model2	Model3	Model4	Model8	Model9	Model10	Model13
KH	103.12	102.17	102.67	103.12	125.21	170.46	125.38	103.45
GN	98.54	96.61	97.50	98.54	94.96	111.15	95.47	99.11
VD	111.34	109.61	110.31	111.34	104.46	125.02	104.95	111.76
SK	95.56	93.24	93.99	95.56	84.36	77.40	85.09	96.19
BF	77.42	72.15	73.60	77.42	114.78	264.23	114.68	78.58
CO	65.54	60.93	61.75	65.54	133.03	282.26	132.81	69.21
RK	113.54	115.56	115.54	116.30	119.36	185.69	119.67	114.09

Table 20. Model set 1 trial 3 index values (starting phase)

Subject	Model 1	Model 2	Model 3	Model 4	Model 8	Model 9	Model 10	Model 13
KH	94.64	94.95	95.77	94.65	104.54	129.07	104.96	95.13
GN	111.02	110.12	111.01	111.02	101.76	96.95	102.38	111.60
VD	125.79	122.02	122.47	125.79	104.21	95.38	104.56	126.05
SK	131.00	129.06	130.04	131.00	126.68	119.24	127.77	131.97
BF	115.55	112.57	113.35	115.55	170.85	297.79	171.20	116.31
CO	73.83	71.91	71.97	73.83	149.77	290.04	149.27	73.10
RK	103.47	106.20	106.18	106.89	103.73	173.10	103.84	104.12

Table 21. Model set 1 trial 4 index values (constant motion phase)

Subject	Model 1	Model 2	Model 3	Model 4	Model 8	Model 9	Model 10	Model 13
KH	86.44	87.68	87.67	86.44	114.24	159.07	114.35	86.44
GN	124.39	122.69	123.49	124.40	133.45	148.81	133.97	125.03
VD	88.48	83.99	84.08	88.48	82.38	106.91	82.87	88.67
SK	111.46	108.40	108.92	111.46	106.36	110.67	107.17	112.02
BF	145.61	144.75	143.57	145.61	217.35	347.14	217.11	144.76
CO	84.37	82.60	82.06	84.37	147.89	269.06	147.47	83.66
RK	164.82	165.23	165.22	166.03	213.21	290.68	213.52	165.39

Table 22. Model set 1 trial 5 index values (constant motion phase)

Subject	Model 1	Model 2	Model 3	Model 4	Model 8	Model 9	Model 10	Model 13
KH	98.87	98.08	98.1	98.87	81.36	105.27	81.57	98.94
GN	97.39	93.59	93.68	97.39	96.91	116.15	97.44	97.6
VD	83.71	79.82	79.64	83.71	89.23	119.77	89.75	83.57
SK	119.06	118.21	118.63	119.06	121.09	125.48	121.51	119.46
BF	116.86	113.75	113.6	116.86	128.35	218.27	127.83	116.89
CO	106.48	104.45	104.46	106.48	112.45	238.95	111.62	106.42
RK	116.68	117.03	117.02	117.43	145.75	222.59	145.65	116.85

Table 23. Model set 1 trial 6 index values (constant motion phase)

Subject	Model 1	Model 2	Model 3	Model 4	Model 8	Model 9	Model 10	Model 13
KH	91.01	89.92	90.09	91.00	115.98	152.42	116.34	91.09
GN	94.57	95.31	96.11	94.58	101.20	111.27	102.13	95.22
VD	75.81	74.28	74.50	75.81	81.46	111.19	81.71	76.03
SK	113.62	113.26	113.66	113.62	109.40	109.32	110.35	114.09
BF	128.17	126.44	125.54	128.16	149.52	226.45	148.78	127.39
CO	74.40	74.24	74.37	74.40	119.57	227.84	119.32	74.56
RK	119.61	115.92	115.93	116.15	162.95	240.34	162.63	119.05

Table 24. Model set 1 trial 7 index values (stopping phase)

Subject	Model 1	Model 2	Model 3	Model 4	Model 8	Model 9	Model 10	Model 13
KH	109.02	108.23	109.13	109.02	118.85	144.47	119.36	109.61
GN	79.16	73.48	74.27	79.16	89.14	111.54	90.04	79.93
VD	98.25	92.4	91.8	98.25	59.64	92.4	59.63	97.88
SK	110.17	105.9	105.83	110.17	103.6	112.85	103.75	110.19
BF	133.47	129.2	128.04	133.46	186.28	322.92	186.04	132.8
CO	88.52	87.81	89.19	88.52	157.41	275.9	158.65	89.77
RK	98.31	96.79	96.79	97.23	119.03	174.91	119.08	98.34

Table 25. Model set 1 trial 8 index values (stopping phase)

Subject	Model 1	Model 2	Model 3	Model 4	Model 8	Model 9	Model 10	Model 13
KH	78.97	78.96	78.69	78.97	87.34	122.47	87.27	78.81
GN	115.97	108.51	109.62	115.98	131.75	170.39	132.69	116.97
VD	86.93	80.76	80.76	86.93	96.64	149.72	97.23	87.13
SK	105.58	101.89	102.23	105.58	109.55	128.79	110.33	105.93
BF	120.22	118.39	117.72	120.22	164.14	285.69	164.03	119.77
CO	100.08	102.20	102.28	100.08	174.79	313.79	174.88	100.00
RK	142.42	127.50	127.52	130.81	132.64	203.64	132.78	141.84

Table 26. Model set 1 trial 9 index values (stopping phase)

Subject	Model 1	Model 2	Model 3	Model 4	Model 8	Model 9	Model 10	Model 13
KH	78.97	78.69	77.60	79.60	113.21	170.95	113.48	79.39
GN	90.21	86.49	86.83	90.21	104.34	136.29	104.71	90.6
VD	91.99	85.95	85.42	91.99	87.25	152.73	87.2	91.66
SK	72.88	69.12	69.61	72.88	93.37	128.89	93.83	73.44
BF	93.49	93.74	94.19	93.49	197.95	336.41	197.79	93.79
CO	118.73	113.65	112.1	118.73	197.73	332.6	197.6	117.45
RK	112.87	102.01	102.01	104.35	133.90	222.68	134.28	112.54

Table 27. Model set 1 average[a] starting index values

Subject	Model 1	Model 2	Model 3	Model 4	Model 8	Model 9	Model 10	Model 13
KH	91.14	90.77	91.39	91.13	103.99	133.27	104.38	91.51
GN	99.88	98.26	99.18	99.89	91.48	83.79	92.27	100.52
VD	105.06	101.74	102.35	105.06	92.24	87.65	92.73	105.42
SK	103.07	101.48	102.24	103.08	96.98	87.85	97.77	103.76
BF	60.14	55.37	57.03	60.23	99.52	216.57	99.2	61.63
CO	51.27	47.97	48.48	51.27	113.93	254.21	113.27	53.33
RK	86.26	88.05	88.03	88.98	91.06	165.44	91.17	86.75

a Observed and predicted force profiles were averaged across the three trials of each phase. Index values were then calculated for the averaged data.

Table 28. Model set 1 average constant motion index values

Subject	Model 1	Model 2	Model 3	Model 4	Model 8	Model 9	Model 10	Model 13
KH	75.26	75.37	75.45	75.26	93.90	130.68	94.12	75.33
GN	92.83	89.70	90.35	92.83	92.71	101.21	93.41	93.40
VD	63.82	59.03	58.98	63.82	49.01	62.88	49.82	63.93
SK	106.72	105.50	105.83	106.72	97.84	88.74	98.33	107.07
BF	101.70	97.46	95.79	101.70	127.47	225.41	127.04	100.46
CO	66.87	63.54	62.81	66.87	98.79	212.64	98.43	66.19
RK	102.28	100.55	100.55	100.82	104.40	126.66	103.88	101.99

Table 29. Model set 1 average stopping phase index values

Subject	Model 1	Model 2	Model 3	Model 4	Model 8	Model 9	Model 10	Model 13
KH	61.33	63.38	63.34	61.33	87.27	122.65	87.54	61.23
GN	86.36	79.97	81.01	86.37	99.64	125.58	100.68	87.25
VD	80.65	74.18	73.58	80.65	63.41	118.02	63.61	80.30
SK	82.85	77.65	77.87	82.85	82.20	104.40	82.99	83.19
BF	98.54	89.76	88.8	98.54	130.50	273.02	130.67	98.02
CO	77.24	72.82	72.69	77.24	117.18	232.48	117.11	77.02
RK	119.91	102.98	102.99	107.07	87.70	150.17	88.84	86.63

Table 30. Model set 2 index values for trial 1

Subject	Model 21	Model 22	Model 23	Model 24
VD	112.03	104.23	94.25	86.10
SK	72.99	67.70	61.22	66.77
BF	96.78	96.79	96.87	96.99
RK	102.34	97.40	98.10	103.45

Table 31. Model set 2 index values for trial 2

Subject	Model 21	Model 22	Model 23	Model 24
VD	97.53	94.05	91.54	95.47
SK	71.94	64.36	66.92	80.16
BF	77.87	77.83	77.91	78.23
RK	104.89	100.91	99.75	102.96

Table 32. Model set 2 index values for trial 3

Subject	Model 21	Model 22	Model 23	Model 24
VD	106.05	102.83	91.61	84.23
SK	107.57	98.13	100.93	113.22
BF	116.10	116.08	116.08	116.10
RK	90.80	89.38	88.74	94.43

Table 33. Model set 2 index values for trial 4

Subject	Model 21	Model 22	Model 23	Model 24
VD	82.38	83.85	83.43	84.88
SK	108.72	100.77	105.19	111.66
BF	144.89	144.84	144.62	144.22
RK	191.77	181.73	187.23	196.16

Table 34. Model set 2 index values for trial 5

Subject	Model 21	Model 22	Model 23	Model 24
VD	91.83542	82.76345	85.73133	92.17
SK	120.8852	108.7694	116.049	128.13
BF	116.8182	116.7709	116.7913	116.85
RK	118.2548	116.1066	122.426	131.34

Table 35. Model set 2 index values for trial 6

Subject	Model 21	Model 22	Model 23	Model 24
VD	81.31	78.95	86.49	95.68
SK	102.46	94.15	96.58	109.13
BF	127.65	127.64	127.61	127.63
RK	136.61	134.14	142.46	151.82

Table 36. Model set 2 index values for trial 7

Subject	Model 21	Model 22	Model 23	Model 24
VD	72.54	99.81	101.18	102.87
SK	115.71	122.33	133.45	147.55
BF	132.93	132.73	132.57	132.33
RK	115.47	109.36	113.67	119.33

Table 37. Model set 2 index values for trial 8

Subject	Model 21	Model 22	Model 23	Model 24
VD	82.12	83.48	82.82	84.45
SK	111.33	101.71	104.13	111.18
BF	119.76	119.86	119.87	119.88
RK	123.44	139.20	139.32	139.93

Table 38. Model set 2 index values for trial 9

Subject	Model 21	Model 22	Model 23	Model 24
VD	73.96	89.88	93.58	98.88
SK	111.89	82.49	91.86	102.30
BF	93.98	93.73	93.73	93.73
RK	101.54	113.48	115.85	119.29

Table 39. Model set 2 average starting index values

Subject	Model 21	Model 22	Model 23	Model 24
VD	90.78	86.76	77.92	70.78
SK	74.45	68.80	62.62	61.63
BF	55.19	55.21	55.44	55.94
RK	74.84	72.56	74.41	80.65

Table 40. Model set 2 average constant motion index values

Subject	Model 21	Model 22	Model 23	Model 24
VD	53.06	59.37	61.84	67.76
SK	87.07	85.58	84.01	86.35
BF	93.74	93.75	93.68	93.59
RK	109.90	114.52	121.02	128.07

Table 41. Model set 2 average stopping index values

Subject	Model 21	Model 22	Model 23	Model 24
VD	56.09	79.78	80.87	82.75
SK	87.37	82.30	90.68	100.78
BF	98.01	97.97	97.95	97.93
RK	96.29	117.55	117.76	118.16

Table 42. Experimental subject group model 23 for starting phase

	Trial #			
Model 23	**1**	**2**	**3**	**Mean**
KH	No data	143.07	104.47	106.61
GN	104.93	86.88	76.00	62.96
CO	73.25	60.91	83.98	45.96

Table 43. Experimental subject group model 22 for constant motion phase

	Trial #			
Model 23	**4**	**5**	**6**	**Mean**
KH	113.04	85.66	109.81	92.34
GN	123.26	95.022	102.79	81.95
CO	121.56	119.25	87.49	77.80

Table 44. Experimental subject group model 21 for stopping phase

	Trial #			
Model 21	**7**	**8**	**9**	**Mean**
KH	96.19	103.43	100.16	74.07
GN	76.00	131.99	112.46	96.93
CO	101.26	113.74	159.45	59.19